Geology, geochemistry and mineralisation of the Erongo Volcanic Complex, Namibia

F. Pirajno
Department of Geology, Rhodes University, P.O.Box 94, Grahamstown 6140, Republic of South Africa

Accepted 15 April 1990

The Erongo Volcanic Complex (EVC) is one of a number of anorogenic complexes of the Damaraland Alkaline Province in west-central Namibia. The EVC is a well-preserved caldera-like volcano-plutonic structure of late Jurassic age. Geological mapping, and studies of the petrology, geochemistry and mineralised systems have permitted the reconstruction of the geological evolution of the Complex. The history of the EVC commenced with the outpouring of basaltic lavas on a basement formed by fault-bounded blocks of late Proterozoic rocks of the Damara sequence, overlain by clastic sediments of Karoo age. The lavas reached a thickness of 300m. The next eruptive phase comprised three volcano-plutonic events, each culminating with voluminous eruptions of pyroclastic flows. The Erongorus event, consisted of intermediate to felsic ash-flow tuffs and intercalated mafic lavas. This was followed by the Ombu event characterised by the uprise of granodioritic magma and its vesiculation and fragmentation, from a central vent, producing a series of ignimbrites of dacitic to rhyodacitic composition. The third event was characterised by the intrusion of the Erongo granite, and its possible venting through ring fractures along the outer periphery of the EVC. Rheomorphic rhyolitic rocks, probably ash-flows, are the effusive products. Collapse of the volcanic structure and the formation of a caldera was perhaps coeval with this event. The emplacement of the Erongo granite also resulted in widespread B-metasomatism and locally greisen-type W, Sn, F, and Be mineralisation. Geochemically, the pyroclastic rocks show some similarity with the quartz-latites of the Etendeka Formation, whereas the intrusive rocks (Ombu granodiorite and Erongo granite) have peraluminous chemistry with A-type affinities. The last magmatic event to affect the EVC was the intrusion of lamprophyre dykes and undersaturated alkaline rocks.

Die Erongo Vulkaniese Kompleks (EVK) is een van 'n aantal anorogeniese komplekse van die Damaraland Alkaliese Provinsie in die wes-sentrale deel van Namibië. Die EVK is 'n goed bewaarde, kaldeire-agtige, vulkanoplutoniese struktuur van Laat-Juraouderdom. Geologiese kartering, en bestudering van die petrologie, geochemie en gemineraliseerde stelsels is uitgevoer. Die resultate van hierdie werk het die rekonstruksie van die geologiese ewolusie van die Kompleks moontlik gemaak. Die geskiedenis van die EVK het begin met die uitvloei van basaltiese lawas op 'n vloer gevorm deur verskuiwingsbegrensde blokke van Laat-Proterosoïese gesteentes van die Damara Opeenvolging, wat weer oorlê is deur klastiese sedimente van Karoo-ouderdom. Die lawas het 'n dikte van 300 m bereik. Die volgende eruptiewe fase het drie vulkanoplutoniese gebeurtenisse behels, wat elk gekulmineer het met volumineuse erupsies van piroklastiese vloeie. Die Erongorusgebeurtenis het bestaan uit die uitvloei van intermediêre tot felsiese asvloeituwwe en tussengelaagde mafiese lawas. Dit is gevolg deur die Ombugebeurtenis wat gekenmerk is deur die opstyg van granodioritiese magma uit 'n sentrale opening, die vesikulasie en fragmentasie daarvan en die lewering van 'n reeks ignimbriete van dasitiese tot riodasitiese samestelling. Die derde gebeurtenis is gekenmerk deur die indringing van die Erongograniet, en die moontlike uitbars daarvan deur kringbreuke langs die buiteperiferie van die EVK. Reomorfiese riolitiese gesteentes, waarskynlik asvloeie, is die effusiewe produkte. Instorting van die vulkaniese struktuur en die vorming van 'n kaldeire was miskien kontemporêr met hierdie gebeurtenis. Die inplasing van die Erongograniet het ook uitgeloop op wydverspreide B-metasomatisme en lokale greisentipe W-, Sn-, F-, en Be-mineralisasie. Geochemies toon die piroklastiese gesteentes 'n mate van ooreenstemming met die kwartslatiete van die Etendeka Formasie, terwyl die intrusiewe gesteentes (Ombugranodioriet en Erongograniet) 'n peralumineuse chemie met A-tipe verwantskap het. Die laaste magmatiese gebeurtenis om die EVK te affekteer was die indringing van lamprofiergange en onderversadigde alkaliese gesteentes.

Introduction and regional setting

In southern and southwestern Africa products of intracontinental alkaline magmatism are widespread and represented by a series of igneous complexes including saturated and undersaturated mafic and felsic rocks, carbonatites and kimberlites. These complexes are arranged generally along northeast-trending lineaments, others have northerly alignments. The northeast trends are possibly due to old structures reactivated during the Pan African and Gondwana tectonic events. Marsh (1973) postulated that the northeast trends of the anorogenic complexes may be related to continental extensions of oceanic transform faults (Figure 1). In Namibia and South Africa the intracontinental alkaline complexes are grouped into three major provinces. The Damaraland Alkaline Province and the Luderitz Alkaline Province, are of Mesozoic age (Jurassic-Cretaceous), whereas further to the south the Kuboos-Bremen Line is of Pan-African age (about 550 Ma), and extends across the Orange River between South Africa and Namibia. Known mineral deposits in these intracontinental complexes include porphyry-style Cu-Mo in the Kuboos-Bremen Line (Viljoen *et al.*, 1986, Bernasconi, 1986), hydrothermal SN-W-F and disseminations of REE and Nb minerals in the Mesozoic Damaraland complexes (Pirajno & Jacob, 1987).

The Damaraland Alkaline Province (Figure 1A), comprises at least 15 volcano-plutonic complexes, extending for about 350km, from the Atlantic coast towards the interior, in a general northeast direction (Prins, 1981). The complexes ware emplaced within the intracontinental branch of the Pan-African Damara Orogen, between 190 and 123 Ma ago (Erlank *et al.*, 1984) during the late phases of the Gondwana break-up and following voluminous outpourings of basaltic lavas and ash-flow tuffs of the Etendeka Formation (Milner, 1988; Marsh, 1987; Erlank *et al.*, 1984). The Damaraland complexes represent eroded remnants of volcanic centres, characterised by dominant explosive activity.

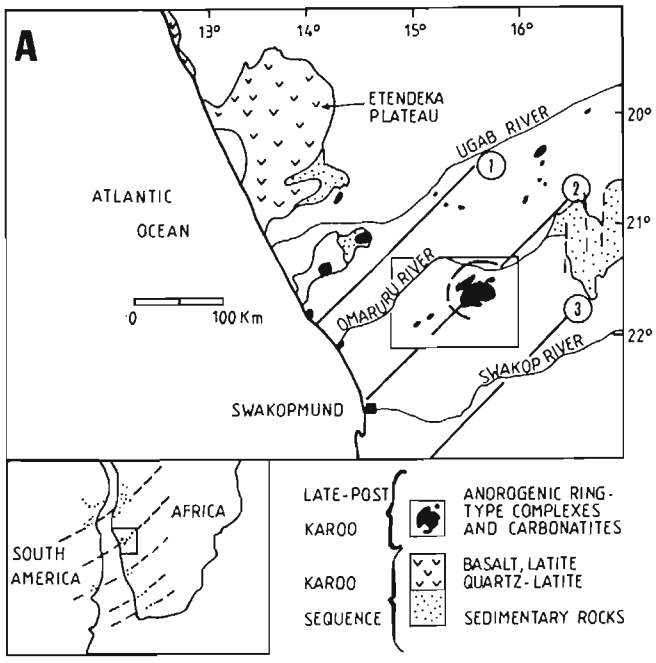

Figure 1(A) Generalised geological map showing distribution of Karoo Sequence rocks and anorogenic complexes of the Damaraland Alkaline Province. The inset shows the possible relationship of the anorogenic ring complexes with transform directions in the South Atlantic (after Marsh 1973). The Erongo Volcanic Complex is in the boxed area, which is also the approximate outline of the LANDSAT imagery.

This paper focusses on the geology of the Erongo Volcanic Complex (EVC), one of the better preserved volcano-plutonic complexes of the Damaraland Alkaline Province. The EVC was first studied by Cloos (1911), and much later by Blümel *et al.* (1979), while brief mention of the Complex is made in the works of Siedner and Miller (1968) and Martin *et al.* (1960). The present work consisted of geological mapping at the scale of 1:50 000, using topographical maps and aerial photographs. LANDSAT imagery aided in the regional interpretation (Figure 1B). Petrological studies were conducted on all lithologies. A limited number of geochemical analyses of selected specimens were made and the results integrated with the analyses published by Blümel *et al.* (1979). Mineral deposits and occurrences related to the Erongo magmatism have been studied by Pirajno & Jacob (1987) and Pirajno & Schlögl (1987) and are briefly described in this paper.

Geology and petrology

Introduction

The EVC is a caldera-like volcano-plutonic structure consisting of mafic lavas, felsic products and subvolcanic intrusive rocks. Two major phases are recognised. An earlier mafic phase characterised by basaltic volcanism and a later felsic phase, characterised by three distinct volcano-plutonic events. The earliest felsic volcanism was the Erongorus event, characterised by a sequence of ash-flow tuffs of intermediate to felsic composition, with intercalated basaltic lavas at the base. This was followed by the intrusion of a granodioritic melt and the emplacement of a series of rhyodacitic ignimbrites from a central vent area (Ombu event). The third eruptive event included the intrusion of an A-type granitic melt (Erongo event). It is considered possible that this granite (Erongo granite) vented at surface giving rise to the third and uppermost sequence of pyroclastic rocks. Finally, lamprophyre dykes and undersaturated mafic plugs were emplaced into the pyroclastic pile. A regional view and a geological map of the EVC are shown in Figures 1 and 2, respectively. Stratigraphic relationships between rock types and the volcanic history of the Complex are diagramatically shown in Figure 12.

Rocks of the mafic phase

Basaltic lavas

The Erongo volcanism began with voluminous effusions of basaltic lavas. The lavas probably formed a broad platform whose areal extent may have exceeded their present-day distribution, as indicated by the isolated lava remnants at Krantzberg in the northeast. The feeders of the basaltic rocks are not known, but it can be conjectured that they were derived from fissures rather than central vents. A number of radial mafic dykes and a cone sheet of olivine dolerite outcropping to the west and north could have been some of the feeders of the Erongo basaltic volcanism.

The EVC basaltic rocks form a succession of lava flows reaching a maximum thickness of up to 300m. The lavas were erupted on a basement formed by fault-bounded blocks of granites and metasediments of Damaran age, on which immature clastic sediments had accumulated on fault scarps and small basins. These sedimentary rocks are part of the Karoo Sequence and they are not treated further in this paper as they have been studied by Hegenberger (1988). The Erongo basaltic lavas were, therefore, deposited in places directly on Damaran rocks and in other places on the Karoo sediments. The present-day extent of the lavas is that of a nearly continuous annular distribution of outcrops, overlain by the later pyroclastic sequences. This basaltic volcanism appears to have been entirely subaerial. Only at one locality (Omandumba West) equivocal round structures in the lavas are suggestive of interaction with water.

Limited geochemical and petrological data support the contention that the lavas originated from different magmatic reservoirs at different levels or, perhaps different batches of magmas rising periodically into the feeding system. In the field the diversity of the lavas is exemplified by a number of type areas. One of these areas is in the northwest (Omandumba West and East farms), where the lavas overlie basement rocks, and occur as flows less than 10m thick, intercalated with both Karoo sediments and pyroclastic rocks of the Erongorus event, over a stratigraphic interval of approximately 100m. It can be surmised that this was an area where the basement faults were active and formed an irregular topography. From field evidence it appears that the basaltic volcanism continued intermittently along the active faults after the first eruption of pyroclastic material. On the farm Erongorus an uninterrupted sequence of lava flows can be observed overlying a well-developed clastic unit of the Karoo Sequence (Krantzberg Formation, Hegenberger, 1988). At the farm Brabant, along the southern margin of the EVC, the lavas overlie Damaran metasediments (Kuiseb

schist and pegmatites), and form a pile approximately 200m thick (Figure 3). In the upper portions, lava flows become very fine grained and trachytic in composition, and intercalate with tuff rocks of mafic to intermediate composition. The latter are included into and represent the start of the Erongorus pyroclastic sequence. These uppermost basaltic rocks are interpreted as heralding a change towards more acidic magma-types leading up to the ash-flow tuffs of the Erongorus sequence. In the southeast (Nieuwoudt farm), the lava flows attain thicknesses of 300m, they overlie Karoo sediments (Lion's Head Formation, Hegenberger, 1988), and have been intruded by the Ombu granodiorite (OG) along their northern contact.

Petrography

The EVC lavas are fine-grained, amygdaloidal, quartz-normative pyroxene basalts and olivine basalts. They contain plagioclase, clinopyroxene, olivine, Fe-Ti oxides, and locally orthopyroxene. Alteration of both groundmass and phenocrysts is common. In the Nieuwoudt area the basaltic rocks contain olivine and plagioclase with compositions ranging from An_{56} to An_{62} (labradorite). Disseminated small grains of olivine and orthopyroxene are present in an altered intergranular to glassy groundmass consisting of plagioclase microlites, sericite, red-brown biotite (Fe-rich ?),chlorite, epidote, and opaques. In the Erongorus area the lavas contain plagioclase ranging from An_{45} to An_{64} (andesine-labradorite), pyroxene grains, and disseminated opaques in an altered groundmass composed of actinolite, chlorite, red-brown biotite, epidote, sericite, quartz, and carbonate. The alteration mineral assemblage of actinolite-biotite-epidote is probably due to thermal metamorphism induced by the intrusion of the Erongo granite. In places geodes are present and contain crystals of quartz amethyst, epidote, and zeolites. In the Omandumba West area basaltic rocks contain plagioclase microlites and laths with An_{55-60} compositions, set in a chloritised groundmass with opaques and epidote grains.

Cone sheet and dykes

A circular intrusion of olivine-dolerite, well visible on LANDSAT imagery (Figure 1), outcrops to the north and west of the EVC. This intrusion is about 200m wide in places (Watson, 1982) and has an inferred diameter of about 40km. This olivine-dolerite has a modal composition of 67% labradorite, 25% augite, 5,7% olivine, 1,7% opaques, and 0,3% other minerals (Watson, 1982). The composition of

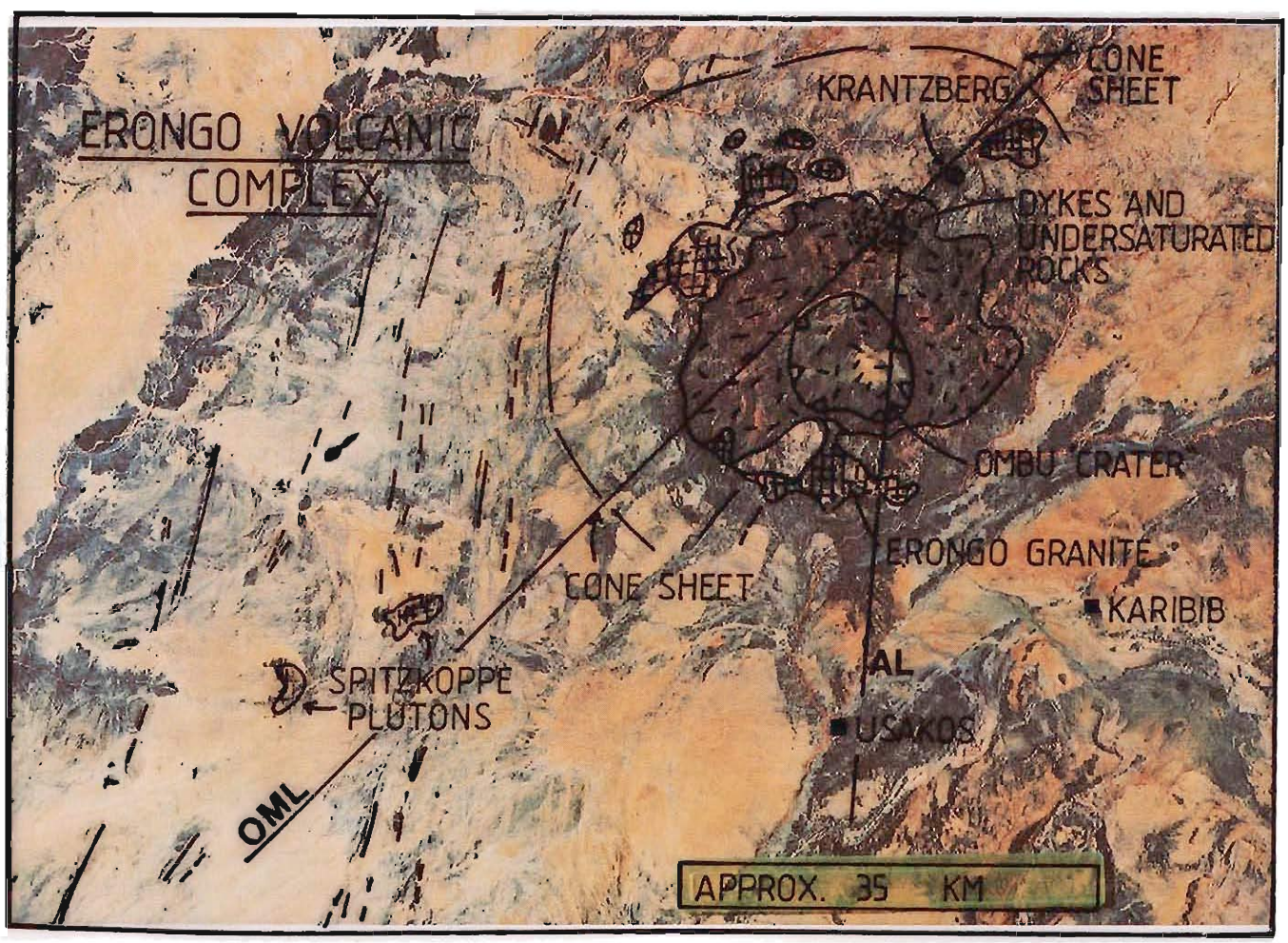

Figure 1(B) (Bands 5 and 7). The interpretation overlay shows the outline of the Complex, outcrops of the Erongo granite (hatches) and the cone sheet. Dashes indicate intracaldera mafic lavas and felsic pyroclastics. Also shown is the area of lamprophyre and undersaturated mafic intrusions in the north of the Complex, at the intersection of the Omaruru Lineament (OML) and the Abbabis Lineament (AL). To the west and southwest of the Complex is a major north-northeast-trending dyke swarm (black lines).

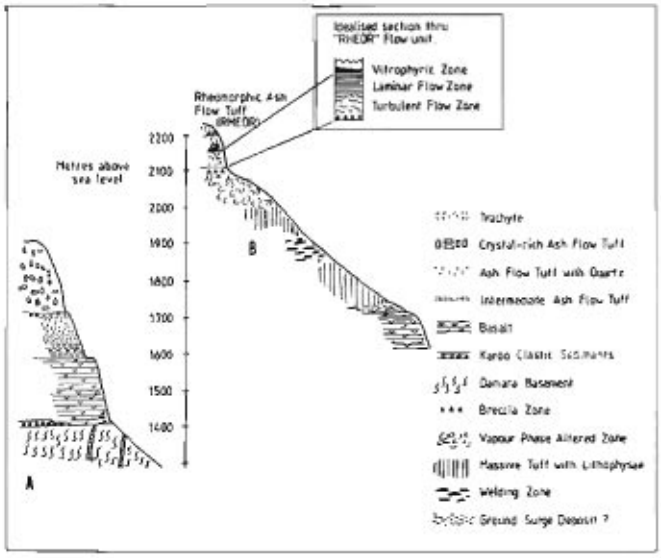

Figure 3 Sketch of sections through EAFT sequence at Brabant (A) and Erongorus (B). In the latter area the EAFT sequence is overlain by RHEOR rocks (shown in the inset).

labradorite is An_{64-68}, olivine occurs as small subhedral crystals with incipient alteration to serpentine and chlorite. Augite forms large plates and imparts to the rock a typical ophitic texture. Aldrich (1986) reported that a prominent magnetic anomaly is associated with this circular intrusion. Based on a qualitative interpretation of its geomagnetic signature, Aldrich (1986) proposed that the intrusion is inclined towards the EVC. If Aldrich's interpretation is correct then the intrusion is probably a cone sheet.

Mafic dykes, thought to be coeval and associated with the basaltic lavas, occur in the south, where they intrude Damaran rocks and Karoo sediments and appear to be radially disposed with respect to the EVC. A thin section of one of these dykes shows an intergranular texture with clinopyroxene, partially altered to red-brown biotite, and plagioclase of An_{55} composition. In the northeast near Krantzberg, a number of dykes have northerly trends and also intrude basement rocks and appear to be cut off by the pyroclastic rocks. A major dyke swarm present in the north and northeast is discussed later.

Rocks of the felsic phase

Introduction

The EVC is characterised by voluminous pyroclastic deposits ranging in composition from andesitic to rhyolitic but more commonly rhyodacitic (Figure 8, A-B). Based on stratigraphic and petrographic evidence they are subdivided into three sequences, namely : Erongorus ash-flow tuff (EAFT), Ombu ash-flow tuff (OAFT) and rheomorphic rhyolitic rocks (RHEOR), (see legend of Figure 2).

There are many different aspects of the EVC ash-flow tuffs in terms of their geometry, stratigraphy, microscopic and macroscopic structures, outcrop scale features, and alteration patterns. Also many of the features change according to the the vertical and/or lateral position within a given cooling unit and its distance from the vent area. Accordingly, it is very difficult to establish a valid set of characteristics which can be generally applied. Nevertheless, from the observation of outcrops, field and stratigraphic relationships, and a comprehensive study of thin sections, certain general patterns do emerge. It is also important to state at the outset that it is difficult, if not impossible in most cases, to recognise in the field individual flow units formed in a single event. This difficulty stems in part from the nature of the outcrops, which are usually broken, covered by scree and/or vegetation, and in part to the fact, that no substantial time breaks occurred between eruptions. Therefore, it is only cooling units (Fischer & Schmincke, 1984) that can be recognised with some degree of confidence. Generally, the boundary between two cooling units is marked by the erosion of the more brecciated, friable and softer upper parts of the underlying unit. In all cases, no intervening palaeosols or sedimentary material were noted, indicating that the pyroclastic eruptions fairly rapidly succeeded one another.

Erongo ash-flow tuff sequence (EAFT; Erongorus event)

Distribution and field relationships

The EAFT rocks constitute the lowermost and first explosive event of the Erongo magmatism. The EAFT has only juvenile material, almost no lithics and was rich in volatiles. The EAFT occupies areas to the west, northwest and north of the Complex, with some small and proximal erosional remnants occurring in the south (Brabant farm). Although the EAFT overlies the basaltic lavas, at Omandumba West and Brabant EAFT basal units intercalate with lavas. The EAFT rocks are overlain by the Ombu ash-flow tuff (OAFT), but in the Omandumba West farm, gabbroic sills occur along the contact between the two pyroclastic sequences.

The base of the sequence in the Brabant farm (near vent area?) is characterised by tuffs, of mafic to intermediate composition, and intercalated lavas with thicknesses of between 20 and 100m. These rocks herald the change from basic and effusive fissure eruptions to a central explosive and acidic volcanism which culminated with large eruptions of ash-flow tuffs. In the west of Brabant farm (Figure 3, A–B) this basal sequence is made up of dark-grey, featureless, strongly welded, massive and aphanitic pyroclastic units intercalated with lava flows of trachytic and basaltic composition. The lavas appear to be welded with the pyroclastic rocks, so that it becomes difficult to differentiate them. The pyroclastic units become more acidic with stratigraphic height, and this is noticeable by the presence of embayed quartz crystals in the otherwise aphanitic matrix. As previously mentioned, individual flow units can rarely be distinguished, but along steep cliff faces in the western and southern margins (Erongorus and Brabant) of the EVC, distinct horizontal breaks may be interpreted as boundaries between individual pyroclastic and lava flows. If this interpretation is correct then these flow units have thicknesses ranging from a few metres (distal) up to 50m (proximal). Upward in the sequence the cooling units become decisively rhyodacitic in composition and display typical pyroclastic textures. The whole sequence may reach a maximum thickness of 370m at Erongorus, 300m at Brabant, and between 200 and 300m in the northwestern areas (Omandumba).

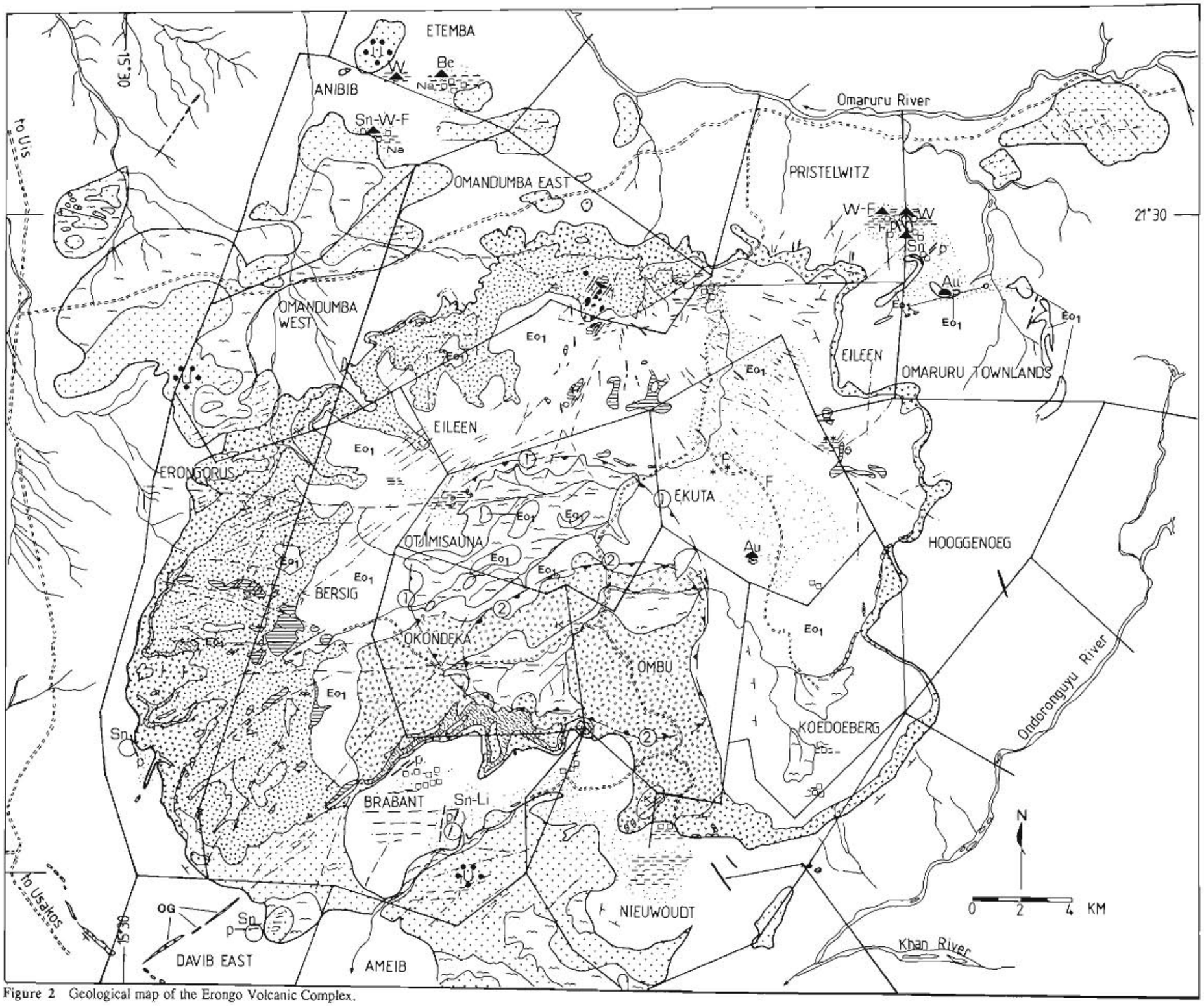

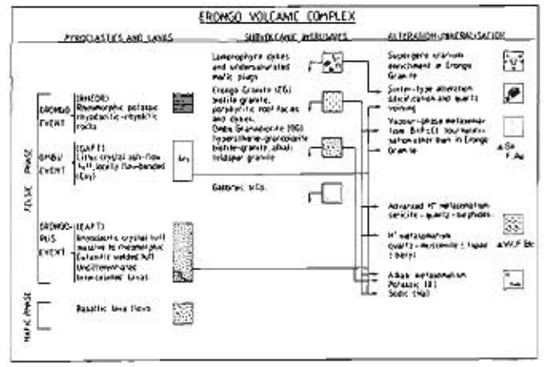

Figure 2 Geological map of the Erongo Volcanic Complex.

Structure and stratigraphy

Complete and most typical sections are found in the Erongorus area (hence the name assigned to this pyroclastic sequence). Generalised type-sections of the EAFT are shown in Figure 3, A–B. In general, EAFT rocks are typically massive, strongly welded, light-grey to brown-purplish (Fe-rich) in colour. In places a basal zone of flow-banded or laminated material is present, which may be interpreted as a ground surge deposit. A zone of strong welding and fiamme structures may be present in the central portions of an EAFT unit. The uppermost portions show intense post-depositional alteration, and have abundant vesicles and/or lithophysae, which give way to brecciated zones near the contact with the next cooling unit. This abundance of lithophysae, vesicles and the lack of lithic fragments are diagnostic of the EAFT units.

In the Omandumba West area sill-like bodies of gabbroic composition, capped in places by basaltic lava flows, occur near the top of the EAFT units, and along their contact with the overlying OAFT pyroclastics.

Petrography

On the basis of mineralogy alone it is difficult to establish the composition of the EAFT rocks. Generally, and taking into consideration the geochemical signature (see Figures 8 and 9), EAFT rocks have compositions ranging from andesitic near the base, to rhyodacitic towards the top.

Examination of thin sections of EAFT rocks at the base of the sequence reveals that, in general, they are characterised by a very fine to fine devitrified groundmass inade up of a felted mass of feldspar microlites, epidote, chlorite, and opaque grains. When examined under high power this groundmass resembles an igneous intergranular to intersertal texture (Figure 4A). Ghosts of feldspars, or other phenocrysts, as well as pumice-like fragments are noticed occasionally. Upward in the sequence an increase in the content of phenocrysts is noted with a concomitant change in the devitrified and microlite-rich groundmass towards a mineralogy and texture approximating those of the OAFT rocks. This devitrified groundmass becomes a graphic intergrowth of quartz and K-feldspar with an increase in K-feldspar phenocrysts, and the appearence of quartz crystals.

In the Erongorus, Bersig, and Omandumba areas, EAFT units show abundant vesicles, fiamme structures, round and embayed quartz crystals, and resorbed K-feldspar phenocrysts. These crystals may reach proportions of between 3 to 7% by volume (Figure 4B). The grey-coloured EAFT rocks of the Omandumba farm show particularly well-developed fiamme structures. On closer examination the fiamme are original collapsed fragments of pumice, recrystallised to aggregates of quartz, chlorite, and sericite or, quartz-clinozoisite +/- clay minerals. Vesicles and lithophysae, are locally abundant especially in the upper zones of the cooling units. Quartz, chlorite, carbonates, and epidote are the most common minerals lining the walls of these cavities.

The gabbroic rocks at the top of the sequence at Omadumba West, are coarse to fine grained, melanocratic to leucocratic. They have a subophitic texture and are composed of olivine, and clinopyroxene plates enclosing plagioclase (An_{47-50}). Groundmass or interstitial material consists of chlorite and disseminated opaques.

Ombu ash-flow tuff sequence (OAFT; Ombu event)

Distribution and field relationships

The Ombu ash-flow tuff (OAFT) is volumetrically the major rock type of the EVC. In the east, northeast, and southeast it overlies basaltic rocks, whereas in the central, west-central areas it overlies the EAFT rocks. In the central and southern areas OAFT rocks surround and grade into its parent subvolcanic intrusive, namely the Ombu granodiorite (OG). OAFT rocks form a typical terraced topography, where each terrace may represent an individual flow unit or, cooling unit.

Structure, stratigraphy, and other characteristics

OAFT rocks have colours ranging from black (usually the

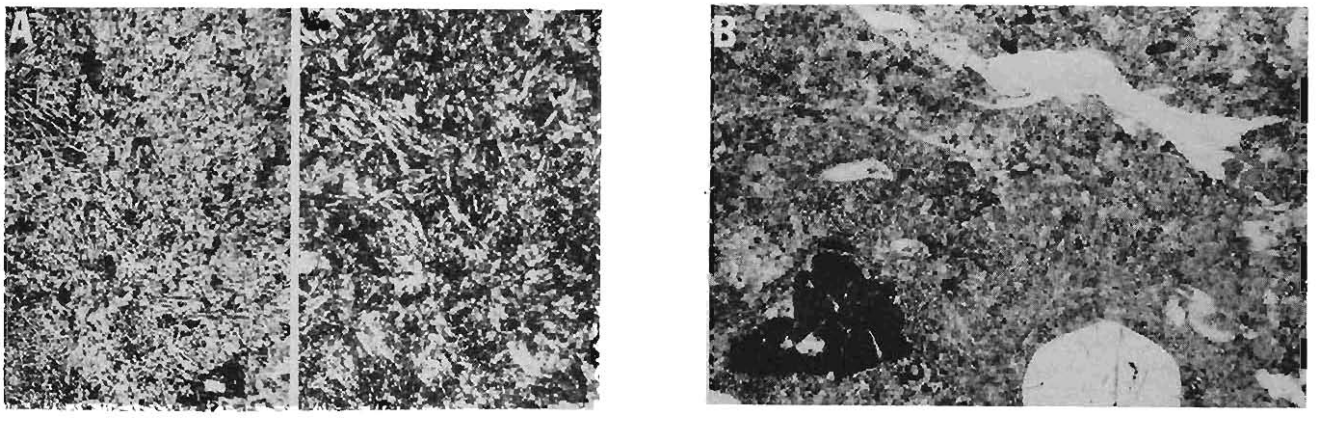

Figure 4 Photomicrographs of EAFT rocks. (A) Pyroclastic material composed of a felted matrix of feldspar microlites, interstitial chlorite, epidote and opaque grains. The specimen is from near the middle of the sequence in the Brabant area (see Figure 2). Photomicrograph at left hand side is in plane polarised light, right hand side is at crossed polars. Field of view for each half photomicrograph is approximately 1,8 mm. (B) Crystal fragments, re-crystallised glass shards, and pumice fragments. Round quartz and resorbed feldspar crystals are set in a brown-greenish devitrified matrix composed of quartz + feldspar + chlorite. Plane polarised light, field of view is 3,5 mm.

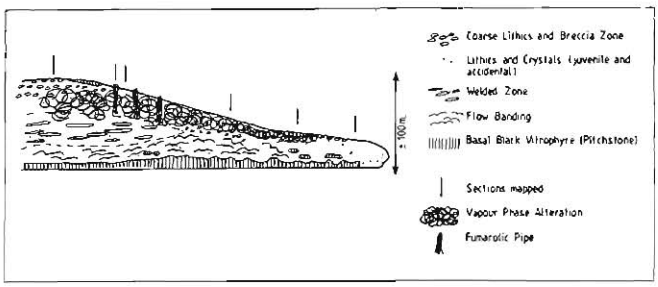

Figure 5 Idealised section through a pyroclastic flow unit of the OAFT sequence. This section was reconstructed using a number of mapped profiles, indicated in the figure by the vertical arrows.

vitrophyric base) to brown and reddish-brown. No pre-ignimbrite plinian basal layers are present, and flow units have no interbedded pyroclastic surges, nor airfall deposits or palaeosols. It is estimated that the OAFT sequence reached thicknesses of at least 500m. Volumes are difficult to estimate; however, using a relationship between caldera size and associated ash-flow tuff (Cas & Wright, 1987) an estimated total of 100km^3 of material could have been erupted.

The OAFT rocks are massive, with locally well-developed flow-banding, crystal-rich to crystal-lithic- rich ignimbrites. Crystals are both juvenile and accidental. Crystal concentrations range from a few volume percent up to 20%. Lithic fragments are abundant and chaotically disposed, ranging in size from a few millimetres to several metres across. Lithics and non-juvenile crystal fragments are derived from the basement and include fragments of quartz-biotite schist, granite and pegmatite. Locally there is an abundance of isolated or aggregated quartz and feldspar crystals of pegmatitic derivation. This implies that fragmentation of basement rocks took place at relatively shallow depths because on the west side of the EVC, the pegmatitic roof zones of late- to post-tectonic Damaran granitoids are exposed at approximately 500m below the present-day floor of the Erongo caldera.

An idealised complete section through an OAFT cooling unit is shown in Figure 5. Four zones can be distinguished, and they are: (1) a basal vitrophyre, followed by; (2) a zone af flow banding; (3) a central area of densely welded tuff, usually in the thickest part of the unit; and (4) an upper-most zone of vapour-phase altered tuff with coarse lithics, and locally fumarolic pipes. The basal vitrophyric zone has

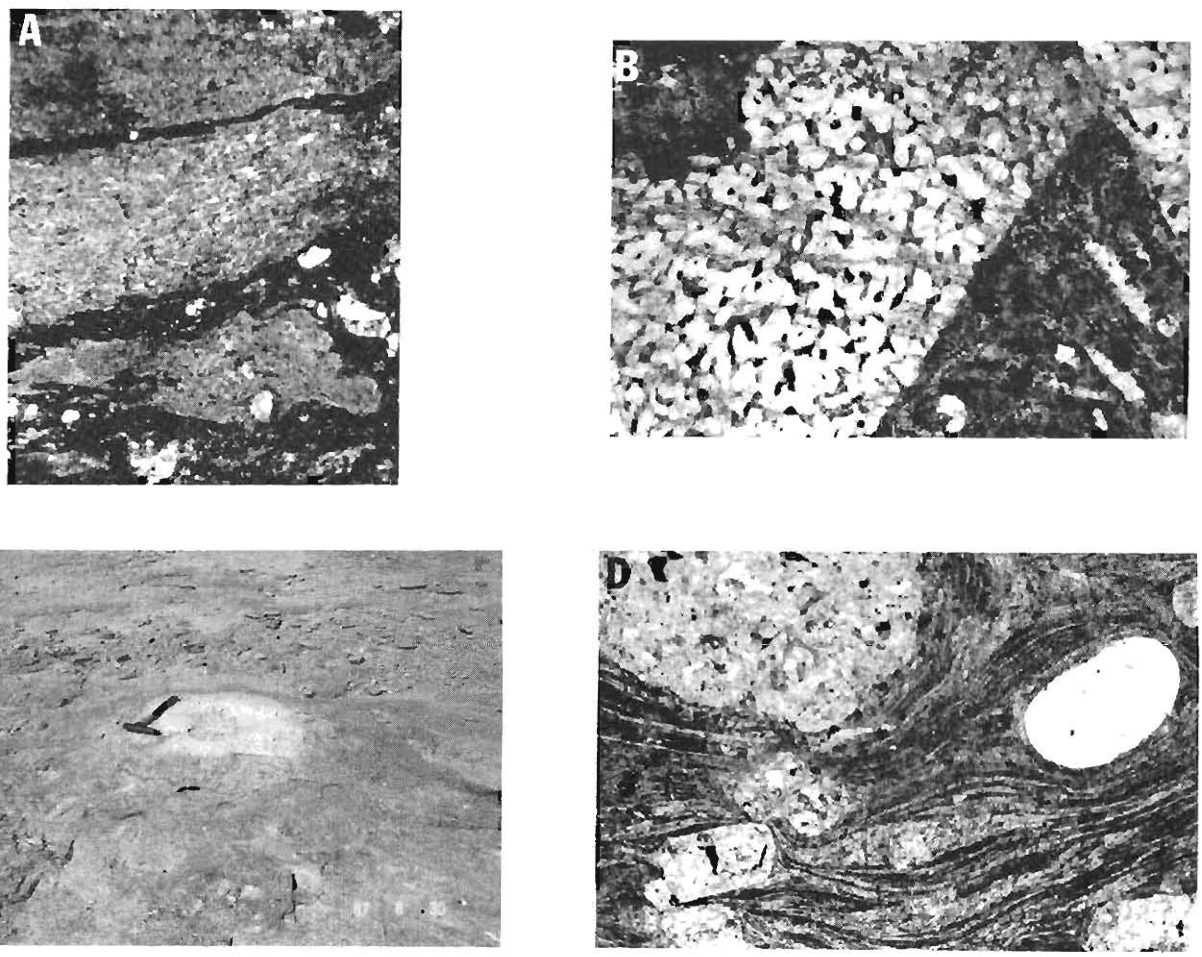

Figure 6 Photomicrographs of OAFT rocks (A, B, and D); all shown in plane polarised light, and field of view 3,5 mm. (A) Welded pumice fragments in devitrified chloritic groundmass. (B) Resorbtion effects on an accidental feldspar crystal (probably from a Damaran pegmatite). (C) Fumarolic pipe in OAFT unit (note silicified halo) outcropping at Ekuta. (D) Well-developed eutaxitic texture in flow-banded unit. Note round quartz crystal, altered and partly resorbed feldspar crystals and stretched out pumice fragments.

variable thickness (from tens of centimetres to several metres) and it consists of dark-grey to black devitrified material, containing up to 15% quartz and K-feldspar. The vitrophyric zone grades upward into the flow-banded tuff, characterised by dark brown to reddish contorted bands with about 10% by volume of crystals. Flow-structures are induced by the movement of the pyroclastic mass, both during its emplacement and after it has come to rest. The central zone of welding is characterised by the presence of flattened pumice and/or lithic fragments (Figure 6A). Welding usually takes place in the thickest parts of the pyroclastic flow and closest to the vent area. High compaction and welding result in extreme stretching and alignment of the glassy fragments, and when this happens a texture known as eutaxitic is formed, which can be readily recognised under the microscope (Figure 6B). The zone of welding passes upward to areas of intense alteration due to the interaction of the pyroclastic material with its own exsolved vapours and fluids. Lithic fragments are particulary abundant in the upper zones, which may reach thicknesses of up to several tens of metres. Another distinctive feature of the OAFT is the presence of fumarolic pipes confined to the upper portions of the cooling unit (Figure 5). The pipes form mound-shaped structures characterised by bleached and silicified haloes. Good examples can be observed in the outcrops along the access road to the Ekuta farm house (Figure 6C).

Petrography

OAFT rocks have compositions ranging from dacitic to rhyodacitic. The mineralogy of the OAFT (excluding accidental crystals) comprises broken crystals of quartz, K-feldspar, plagioclase, and Fe-bearing silicate minerals. The latter are always pervasively altered to chlorite. There is usually more K-feldspar than plagioclase, the latter having compositions ranging from An_2 to An_{22} (albite-oligoclase). Feldspar phenocrysts are usually unaltered, but when altered, sericite, silica, chlorite, carbonate, and Fe oxides are the most common alteration products. The groundmass is made up of devitrification textures characterised by fine granophyric intergrowths of K-feldspar + quartz (trydimite?). Also commonly seen are resorption textures in feldspars resembling myrmekite (Figure 6D). An outstanding feature of OAFT rocks is the devitrification and crystallisation of the groundmass material. There are different degrees and stages of devitrification and crystallisation, a phenomenon which involves the nucleation of quartz and alkali feldspar. A hydration stage, a spherulitic stage, and a granophyric stage were recognised by Lofgren (1971). The OAFT only display the last two with the granophyric stage being the most common. The spherulitic stage is more rarely seen, although a particularly good example can be seen near the Otjimisauna farm house. Spherulites consist of 'bow-tie–shaped' fibrous aggregates of quartz and K-feldspar nucleating around a 'seed', generally a feldspar crystal.

Vapour-phase alteration of OAFT rocks affects large and thick zones usually in the upper sectors of the pyroclastic unit. Characteristically the altered zones have a brown to reddish-brown coloration due to oxidation of Fe. Vugs and cavities may be filled with quartz, fluorite, calcite, and tourmaline. Vapour-phase alteration results in the nucleation of tourmaline rosettes, hematite, chlorite, sericite, muscovite, trydimite, epidote, and carbonates. These minerals usually replace the phenocrysts and form patches and veinlets in the granophyric matrix. Hydraulic fracturing, due to fumarolic activity is locally present. Good examples of hydraulic fracturing can be seen west of the main access road along the Otjiporo river near the Eileen-Pristelwitz farms' boundary. At this locality outcrops display fractures filled with quartz, tourmaline, Fe-oxides, pyrite, sericite, carbonates, and, in places, apatite.

Rheomorphic rhyolitic rocks (RHEOR; Erongo event)

Distribution and field relationships

Outcrops of rheomorphic rhyolitic rocks (RHEOR) occur as scattered isolated erosional remnants. They overlie EAFT rocks in the west and southwest (Erongorus and Bersig farms), and OAFT rocks in the east (Ekuta and Hoeggenoug farms). At the Bersig farm RHEOR rocks locally underlie OAFT units. Near the Bersig farm house RHEOR rocks may have been emplaced in a palaeovalley because outcrops occur some 140m below their contact with EAFT rocks. This low position could also be explained by down-faulting, since a prominent northeast-trending fracture passes through this area, although there is no evidence of displacement. In the north-central area of the EVC (mainly in the Eileen farm), isolated outcrops of a strongly welded, very fine-grained ash-flow tuff overlie the OAFT units and are correlated with the RHEOR rocks.

Field relationships of the RHEOR with the other pyroclastics indicate that they were emplaced at the closing stages of the Ombu event (as they are locally overlain by OAFT units), and that they were emplaced over a rugged topography, with the RHEOR units flowing down into palaeovalleys. The RHEOR may have covered a large area, and as only a few isolated remnants remain their thickness and stratigraphy are incomplete. The present-day outcrops form sequences no more than 100m thick, in which two to four individual flow units may be discerned using the criteria described below. Another problematical feature concerning the RHEOR rocks, is that no feeders have been recognised anywhere within the EVC. For this reason, as well as the limited geochemical constraints explained later, it is proposed that the RHEOR are the extrusive equivalent of the Erongo granite.

Structure and stratigraphy

RHEOR rocks are characterised by fine banding, probably due to mass flowage during and after emplacement. The idealised structure of a RHEOR flow unit is shown in the inset of Figure 3B. An individual flow unit is generally constituted by a basal breccia zone, followed by the flow-banded main body of the unit. The latter consists of a lower section in which the banding is convoluted or folded, and locally may have broken up folded layers. An upper section consists of a fine laminated structure, followed in turn either by a narrow vitrophyric zone, or by a massive and vesicular porphyritic zone. In the Eileen area the welded ash-flow tuffs are yellowish to light-coloured siliceous rocks, with a distinct lenticular appearence. They have well-developed, small, and

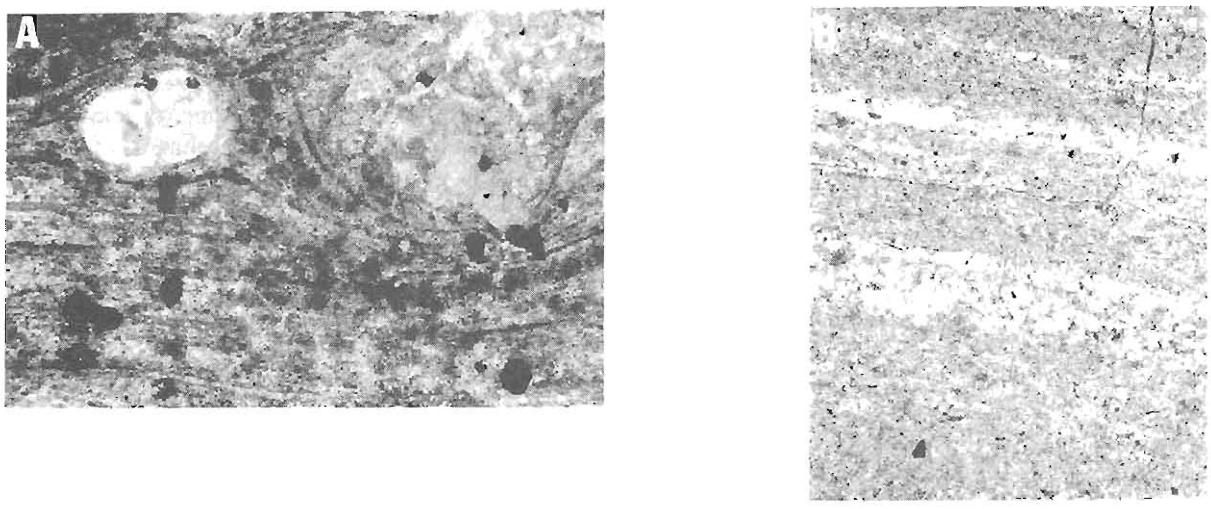

Figure 7 Photomicrographs of RHEOR rocks; plane polarised light, field of view 3,5 mm. (A) Round quartz crystal (upper left) and small lithic fragment showing compaction structure. (B) Fine mm-scale quartz-rich (white) and alkali-feldspar-rich (grey) laminae. Apart from the laminae this rock is characterised by the absence of crystals and of typical pyroclastic structures.

flattened pumice fragments and contain sparse, centimetre-size, lithic blocks, showing compaction structures (Figure 7A). No surge deposits or other intervening material were recognised. Locally, these rocks have acted as a barrier to hydrothermal fluids, because the immediately underlying OAFT rocks show silicification and alteration to sericite, carbonate, and Fe oxides (see Figure 2). The overlying welded tuff rock is fractured and has small quartz vein stockworks.

Petrography

Thin sections of RHEOR rocks from the Ekuta area reveal that they are of rhyolitic composition and contain alkali feldspar phenocrysts and round quartz crystals (Figure 7A). The phenocrysts locally are grouped together imparting the rock a glomeroporphyritic texture. The groundmass has a laminated to fluidal texture and is made up of quartz + alkali feldspar intergrowths, derived from devitrification processes (Figure 7B). Sericite alteration of the feldspars is locally present. Tourmaline occurs as fine overgrowths on the phenocrysts and also along microfractures and flow lines. This tourmaline is probably the result of later introduction of B-rich fluids. In the Bersig and Erongorus areas, the RHEOR rocks are characterised by a very fine-laminated (0,1mm scale) texture. The laminae are alternate quartz-rich +/− sericite and alkali feldspar-rich. Phenocrysts are rare or absent (Figure 7B) and spherulitic textures are occasionally present.

Under the microscope the strongly welded tuffs of the north-central area (Eileen farm), show very fine laminations (mm to fractions of mm scale) (Figure 7A), and small welded pumice fragments in a fine, brown-coloured, devitrified ash material. Small phenocrysts of plagioclase, quartz and K-feldspar may occur disseminated in the devitrified matrix. Sericite and minor pyrite may be present along microfractures.

Subvolcanic rocks

Two major subvolcanic lithologies can be distinguished, namely the Ombu granodiorite (OG) and the Erongo granite (EG).

Ombu granodiorite (OG)

The Ombu granodiorite (OG) outcrops in the south-central area of the EVC, on the farms Ombu, Okondeka, and Bersig. It is exposed for about 14km in an east–west direction, and about 10km in a north–south direction in its eastern portion. This south-central area forms a topographic depression, largely covered by sand and alluvium. To the west, north, and east the OG has gradational contacts with the OAFT rocks, and in places it is very difficult to distinguish the two rocks. Dyke-like bodies of OG material occur in the southwest, outside the EVC along northwest and northeast trends. Petrologically and mineralogically these two lithologies are similar and it is assumed that the OG is the subvolcanic equivalent of the OAFT units. The topographic depression in the Ombu farm is interpreted to be the vent area through which the OG magma rose, vesiculated, and explosively fragmented to give rise to successive eruptions of OAFT units. Along the southern margin the OG intrudes the earlier sequence of EAFT rocks, whereas to the southeast it intrudes the basaltic rocks and the Damara metasediments.

The OG is a coarse- to fine-grained, grey to reddish-brown, massive, granitic rock. Characteristically it is charged with numerous xenoliths of the same nature as the lithic fragments in the OAFT units. They range in size from a few millimetres to several tens of centimetres, and up to 0,5m in places. The xenoliths are represented by fragments of both Karoo and Damaran rocks, with the latter being more frequent.

On the basis of its unaltered mineralogical assemblage and according to the classification of Streckeisen (1976), the OG has compositions ranging from monzo-granite to granodiorite. It is composed of plagioclase, with compositions of An_{30}-An_{42} (oligoclase to andesine), quartz, perthitic orthoclase, hypersthene, red-brown biotite, and Fe-

Ti oxides. Garnet and cordierite are present in places as accessory minerals. Blümel *et al.* (1979) reported an average modal composition of 37% plagioclase, 25% quartz, 21% K-feldspar, 6,8% hypersthene-ferrohypersthene, 5,8% biotite, 3,2% Fe-Ti oxides, 1,2% cordierite and other accessory minerals. They also determined that orthopyroxene and biotite are Fe-rich, and identified an Fe-rich olivine in some samples. The red-brown biotite usually forms rims around hypersthene crystals, and it is thought that this biotite may be replacing the pyroxene during stages of sub-solidus hydrous alteration. In the southern areas (farm boundary between Ombu and Nieuwoudt) the OG forms a prominent hill of pink to reddish-brown-coloured massive rock, with gradational to sharp contacts with the surrounding grey-coloured OG. This rock is essentially composed of a granophyric intergrowth of quartz and K-feldspar. Gradational replacement textures can be observed, from a grey OG with its normal mineralogy as described above, to the reddish-brown OG in which plagioclase, hypersthene, and biotite have been partially to totally replaced by the granophyric assemblage. The K-feldspar of this granophyre rock has a high degree of turbidity, due to fine inclusions of hematite, and is responsible for the reddish-brown coloration of the rock. Granophyric intergrowths of quartz and K-feldspar in evolved igneous systems, can be explained by either pressure quenching, or by cooling and fractionation under volatile-rich conditions (e.g. F, B, H_2O). Experimental work by Pichavant (1981), and Pichavant & Manning (1984), indicates that additions of B or F to the melt may cause sub-solidus microclinisation and silicification (quartz + K-feldspar assemblage), or, in other words, silica and potassic metasomatism. In this work the granophyric variant of the OG is regarded as a product of potassic metasomatism, and this is substantiated by other observations discussed below.

Alteration of the Ombu granodiorite

Hydrothermal alteration of the OG is observed at several localities. Although no spatial pattern was worked out, petrographic evidence indicates two distinct trends of alteration. One trend is characterised by the above-mentioned granophyric texture composed of K-feldspar and quartz with minor overprinting by sericite and chlorite. The other trend is clearly phyllic to propylitic and is characterised by the development of a granular quartz matrix with interstitial K-feldspar and overgrowths of sieve-textured red-brown biotite, chlorite, and non-pervasive to pervasive replacement of plagioclase and pyroxene by sericite and chlorite. With advancing alteration plagioclase and pyroxene phenocrysts are destroyed, and the rock consists of granular quartz, K-feldspar, biotite (also forming cross-cutting veinlets and submicroscopic banding), sericite and chlorite. In places coarser-grained quartz-biotite aggregates have tourmaline overgrowths, which appear to be associated with fine banding and microfracturing. Banding and microfracturing become locally common and are indicative of movement of fluids in the system. Tourmaline occurs as a late-stage mineral.

Erongo granite (EG)

The Erongo granite (EG) occurs as isolated stocks, or plutons of irregular shapes and sizes, distributed all around the Erongo caldera-type structure. EG dykes and minor intrusive bodies also crop out within the central parts of the caldera at Otjimisauna and in the southwest at Bersig. From field evidence it is inferred that the EG may form a continuous body above and around a subsided central block of the Complex and underlying basement rocks. This subsidence could have taken place during, or soon after the extrusion of large volumes of rocks of the felsic phase (RHEOR), causing the collapse of the volcanic superstructure. This is also indicated by the tilt of the basaltic and pyroclastic units, towards the centre of the EVC.

At least two types of EG rocks are recognised. The main type is a massive, coarse-grained, equigranular, sub-solvus biotite granite. An average modal composition, reported by Blümel *et al.* (1979), is: 36% quartz, 33% perthitic orthoclase, 25% albite, 4,5% biotite, and 1,5% accessories (tourmaline, zircon, fluorite, apatite, and topaz). Average modal composition for the EG of the Omaruru Hills pluton to the northeast of the EVC is: 38,5% quartz, 38,5% K-feldspar, 15% albite, 4% biotite and 2% accessories (muscovite, topaz, zircon, tourmaline, apatite, and sphene), (Kujawa, 1986). A finer-grained and porphyritic phase is commonly found as a roof facies in the Otjimisauna area and in the Omaruru Hills pluton. This porphyritic phase is also a subsolvus granite and is represented by a quartz-feldspar porphyry containing K-feldspar, quartz, albite, and biotite. Accessory minerals are muscovite, fluorite, apatite, topaz, zircon, and tourmaline. In the classification of Streckeisen (1976) the EG occupies the field of monzo-granite to sieno-granite, with the more evolved quartz-feldspar porphyry phase tending towards the alkali granite field. In both EG rock types biotite is a late mineral. Muscovite occurs as replacement product of biotite and often is associated with fluorite grains.

A prominent and important feature of the EG is the presence of quartz-tourmaline nests, up to 30cm in diameter, and veins and stringers. The nests are disseminated throughout, are locally very abundant and may coalesce, especially in the roof zones of the stocks, where they may be associated with, and cross-cut, pegmatitic pods and veins. The quartz-tourmaline nests consist of tourmaline, quartz, K-feldspar, plagioclase, biotite, fluorite, apatite, topaz, and rare cassiterite. The nests have an irregular, bleached, reaction zone along their margins, containing quartz and K-feldspar with no biotite. Within the nest, tourmaline replaces biotite and feldspar, or fills open spaces. Tourmaline veins, breccias, and dyke-like bodies, as well as replacement at all scales, are widespread in the country rocks around the EG, up to several hundred metres from its contacts (Pirajno & Schlögl, 1987).

The quartz-tourmaline nests may represent the 'frozen in' incipient stages of a magmatic-hydrothermal system, resulting from localised B-rich fluid separation, following near saturation with respect to volatiles (B,F,Li) in the roof zones of the EG. On the basis of morphological and mineralogical characteristics, at least four types of quartz-tourmaline aggregates can be recognised. They would represent an evolutionary sequence in time and space, from the central portions of the magma body (type I) towards the margins (type II to IV) (Smithies, 1988). At the margins only quartz-tourmaline veins would be present. According to Smithies (1988) this sequence is dictated by progressive

higher degrees of B-saturation, with cooling of the granite body from the margins towards the centre.

Lamprophyre dykes and undersaturated mafic plugs

In the northeast sector of the EVC a swarm of lamprophyre dykes intrudes the EAFT and OAFT sequences. The swarm appears to be associated with a number of undersaturated, nepheline-bearing, mafic plugs, which outcrop in the Omandumba East farm. The plugs are frequently brecciated and contain fragments of Damaran basement rocks, such as granites and pegmatite. It is interesting to note that dykes and the undersaturated mafic plugs occur in an area where two major lineaments intersect (Omaruru and Abbabis lineaments; see Figure 1B), and is coincident with a positive gravity anomaly (Aldrich 1986).

Lamprophyre dykes

Lamprophyre dykes have north–south, east–west, and northwest trends. They are usually highly altered, and show intersertal and glomeroporhyrytic textures. At least two types are distinguished: mica-lamprophyre and olivine-lamprophyre. The former contains clinopyroxene, brown hornblende and a red-brown mica biotite and accessory apatite needles. Feldspar may be totally absent or it may be present as microlites in the groundmass. The groundmass is fine-grained, granular, and may contain clinopyroxene and opaques. Alteration minerals include epidote, chlorite, and carbonate. The olivine-lamprophyre contains phenocrysts of olivine, nepheline, and clinopyroxene in a groundmass consisting of red-brown mica, clinopyroxene, opaques, and carbonate as an alteration product.

Undersaturated mafic plugs

A cluster of about 40 undersaturated mafic plugs and associated dykes cover an area of about 4km^2 along the southern border of the Omandumba farm (Figure 2). The intrusives range in size from 5m to over 100m in diameter. Petrological and geochemical work carried out by Patel (1988) revealed that these intrusive bodies can be subdivided into two groups. They are: (1) plug-like, mesocratic tephrite, phonotephrite, tephriphonolite, and phonolite; and; (2) small (few metres to 10m) dyke-like bodies of basanites, often intruding the plug-like bodies. They are all silica undersaturated, having in excess of 5% normative nepheline.

Phonotephritic rocks are the most abundant rock type in the area. They are medium- to coarse-grained and porphyritic, containing a phenocryst assemblage of clinopyroxene and amphiboles in a groundmass of plagioclase laths, equant nepheline grains, alkali feldspar, clinopyroxene, apatite, and brown mica. Tephrites are fine- to medium-grained mesocratic rocks with a porphyritic to glomeroporphyritic texture. They consist of augite, titanoaugite, olivine, and biotite phenocrysts in a holocrystalline groundmass made up of nepheline and K-feldspar, clinopyroxene, biotite, apatite, and opaques. Tephriphonolites and phonolites are coarse-grained, mesocratic to leucocratic rocks, characterised by the presence of nepheline, alkali feldspar and minor aegirine-augite phenocrysts. The groundmass is generally made up of plagioclase laths, sodalite, carbonate, sphene, cancrinite, and minor amounts of apatite and opaques. Basanite are fine-grained mesocratic rocks containing augite, brown biotite, and occasional olivine. Phenocrysts in a fine-grained groundmass are made up of alkali feldspar microlites, clinopyroxene, biotite, and accessories such as apatite,

Table 1 Major and trace element analyses of basaltic rocks from the Nieuwoudt area. Major elements expressed in weight per cent oxide, trace elements in parts per million. AZ 8766 is a sample from the cone sheet north of the EVC. Analyses performed by ROCKLABS, Pretoria using XRF on fusion discs for major elements and on pressed discs for trace elements. ND = not determined

Sample No	AZ8901A	AZ8949A	AZ8949C	AZ8951	AZ8950B	AZ8766
SiO_2	48,68	55,59	48,26	47,94	50,44	50,54
TiO_2	1,26	1,36	1,12	0,93	1,14	1,36
Al_2O_3	13,42	14,75	13,18	12,29	14,61	16,15
Fe_2O_3	1,66	1,32	1,62	1,61	1,57	1,74
FeO	9,24	7,37	8,99	8,93	8,68	9,63
MnO	0,20	0,14	0,18	0,18	0,17	0,21
MgO	11,18	4,86	10,73	11,35	8,09	5,33
CaO	9,93	7,73	9,05	9,68	10,27	10,51
Na_2O	1,88	3,36	1,82	1,11	2,57	2,59
K_2O	0,59	1,87	0,53	0,81	0,76	0,85
P_2O_5	0,09	0,19	0,08	0,10	0,13	0,06
Cr_2O_3	0,19	0,07	0,20	0,20	0,13	0,06
LOI	0,77	2,64	1,37	4,16	0,21	0,40
Total	99,09	101,25	97,13	99,29	98,77	99,43
Zn	96	90	107	102	109	101
Cu	81	53	78	61	31	128
Ni	287	136	328	426	37	58
Co	45	39	55	60	36	37
Ga	18	11	20	16	21	25
Mo	ND	ND	ND	ND	ND	ND
Nb	6	9	10	8	8	7
Zr	98	119	110	90	113	98
Y	22	22	23	21	27	29
Sr	210	228	183	129	272	242
Rb	15	34	13	18	16	29
U	ND	ND	ND	4	4	ND
Th	ND	ND	ND	ND	ND	ND
Pb	7	10	10	9	12	9
Ba	276	643	219	279	300	204
Sc	38	37	18	28	21	30
Ce	42	19	ND	ND	19	47
Nd	30	ND	ND	ND	20	ND
La	48	ND	25	ND	58	ND
Sn	67	ND	19	ND	18	29
W	ND	ND	ND	ND	ND	ND
As	ND	ND	ND	ND	ND	ND
Ta	ND	ND	ND	ND	ND	ND
Cl	258	93	133	173	101	162
F	100	100	100	100	100	100
Rb/Sr	0,07	0,15	0,07	0,14	0,06	0,12
Nb/Y	0,27	0,41	0,43	0,38	0,30	0,24

Table 2 Major and trace element analyses of basaltic rocks from the Erongorus area. Major elements expressed in weight per cent oxide, trace elements expressed in parts per million. Analytical techniques as in Table 1. ND = not determined; -- = not detected

Sample No	AZ8908A	AZ8908B	AZ8909A	AZ8909B	AZ8909C
SiO_2	53,05	48,01	53,81	59,72	61,46
TiO_2	1,25	1,04	1,21	2,07	1,43
Al_2O_3	12,53	13,25	14,61	12,83	12,64
Fe_2O_3	1,50	1,48	1,63	1,54	1,67
FeO	8,36	8,24	9,05	8,55	8,36
MnO	0,17	0,17	0,22	0,15	0,10
MgO	8,14	10,12	6,46	1,63	0,81
CaO	6,78	8,86	7,46	4,98	4,85
Na_2O	1,76	1,57	1,93	1,53	1,64
K_2O	1,27	1,61	1,24	3,16	3,18
P_2O_5	0,15	0,33	0,13	0,36	0,79
Cr_2O_3	0,12	0,19	0,10	0,04	0,08
LOI	3,86	4,19	1,27	2,01	2,51
Total	98.94	99.06	99.12	98.57	99.52
Zn	99	101	120	115	150
Cu	24	48	23	28	16
Ni	124	247	14	106	11
Co	31	45	20	25	7
Ga	18	15	23	19	21
Mo	--	--	6	--	4
Nb	12	19	19	13	21
Zr	115	112	400	247	405
Y	23	23	63	42	69
Ca	4,84	6,33	5,33	3,56	3,46
Sr	310	385	205	252	224
Rb	30	42	63	42	115
U	--	--	--	--	--
Th	--	4	8	--	19
Pb	14	8	22	13	23
Ba	398	695	1187	834	1260
Sc	36	27	42	35	7
Ce	--	75	115	59	81
Nd	--	27	67	28	47
La	75	65	101	50	69
Sn	23	19	17	22	7
W	ND	ND	ND	ND	ND
Se	ND	ND	ND	ND	ND
As	17	ND	ND	ND	ND
Ta	ND	ND	ND	ND	ND
S	ND	ND	ND	ND	1210
Cl	227	339	126	58	30
F	100	100	132	100	1960
Rb/ Sr	0,10	0,11	0,31	0,17	0,51
Nb/ Y	0,52	0,83	0,30	0,31	0,30

sphene, zircon, and opaques. Megacrysts of clinopyroxene up to 1cm are also present. Disseminated sylphides, pyrrhotite, and pyrite, and Fe-Ti oxides are present in most of these rocks, except the basanites.

The alkaline intrusives are surrounded by a halo of alteration, visible both on aerial photographs and satellite imagery. Field evidence shows that the host pyroclastic rocks are reddened by oxidation of Fe, and nearer the intrusive bodies intense silicification of the pyroclastics is noticeable. In places this silicification forms sinter-like deposits. Also, brecciation of both host pyroclastics and the intrusive plugs is commonly observed. In one place brecciation of the pyroclastic rocks appears to have formed by hydraulic fracturing. Quartz veinlets and open-space filling by quartz crystals suggest circulation of silica-bearing fluids after the emplacement of the intrusives.

Geochemistry

Results of 11 analyses for two suites of basaltic rocks are given in Tables 1 (Nieuwoudt basalts) and 2 (Erongorus basalts). The former are olivine-normative (except for one sample), and contain between 48 and 55,5 wt.% silica (average 50%). The Erongorus lavas are quartz-normative (except for one sample), and have higher silica contents of between 48 and 61,5 wt.% (average 55%).

The mafic lavas of these two areas plot in the subalkaline basalt, basaltic andesite and andesite fields (Figure 8, A–B), with the lavas of the Nieuwoudt area being geochemically less evolved than the Erongorus lavas. It is worthy of note that the single analysis of cone sheet dolerite plots close to the Nieuwoudt lavas, suggesting a possible genetic relationship. In Figure 9 analyses of EVC basalts published by Blümel *et al.* (1979), were incorporated with the present data, and compared with the Etendeka basalts (Milner, 1988; Erlank *et al.*, 1984). These plots indicate that the EVC lavas have a generally more primitive (less evolved) geochemical character than the Etendeka lavas, even though a certain amount of scatter is present indicating that some of the EVC lavas are more enriched in incompatible elements than the Etendeka rocks.

Whole rock major and trace element analyses of selected specimens of pyroclastic rocks (EAFT, OAFT and RHEOR) are given in Tables 3A,B and C. The plots of Figure 8 show that their composition ranges from dacitic to rhyolitic, although the reader must be aware that overprinting by K- and B-metasomatism may have modified the original elemental concentrations. The diagrams shown in Figure 9 were constructed combining these analyses with those published by Blümel *et al.*(1979), as well as data from the Etendeka Formation. The assumption is made that in the work of Blümel *et al.* (1979) the rocks they refer to as rhyodacites correspond to the OAFT, and those called rhyolites correspond to the RHEOR rocks. Taking into consideration their petrological descriptions and the geochemical signature this assumption appears to be fully justified. In this figure the basaltic rocks associated with the EAFT pyroclastics show an enrichment in trace elements (Rb, Ba, Zr, Y) with respect to the Etendeka basalts. The EAFT rocks appear to be geochemically comparable with the Etendeka quartz-latites, except for a strong enrichment in Zr and Y in the EAFT rocks. The EAFT and OAFT tend to group together, however, the paucity of points for the former does not lend this observation enough support. Nevertheless a noticeable difference can be seen in their total Fe contents. Both EAFT and OAFT are enriched in Rb and Ba, and

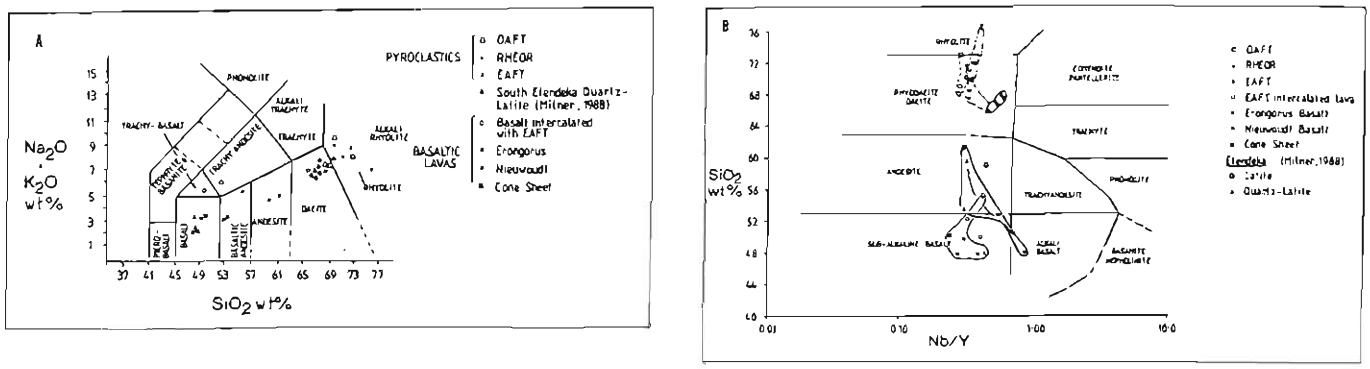

Figure 8 Discriminant diagrams showing compositional fields of EVC lithologies (A = SiO_2 versus $Na_2O + K_2O$; B = Nb/Y versus SiO_2). Latite and quartz-latite rocks from the Etendeka Formation (Milner, 1988), are also plotted for comparison. Diagram A is after Le Maitre (1984); diagram B is after Winchester & Floyd (1977).

depleted in Sr relative to the mafic rocks. Also it is interesting to note that the basaltic rocks intercalated with the EAFT rocks appear to provide a link with those of the Erongorus and Nieuwoudt basalt sequences. The RHEOR rocks, and the rhyolitic rocks of Blümel *et al.* (1979) form a cluster, indicating enrichment in Si, Rb, and depletion in Ba, Sr and Y with respect to the other EVC rock groups.

The AFM plots, shown in Figure 10A, indicate that the three pyroclastic suites are progressively enriched in alkalies and depleted in Fe from the earliest products (EAFT), to the OAFT, through to the RHEOR. At this juncture it must be noted that in comparing Figure 10A with the AFM plot for the subvolcanic rocks (Figure 11C), the RHEOR rocks compare well with the EG, whereas the OAFT rocks overlap both the EG and OG fields, but tend to cluster mostly within the latter's. The EAFT rocks plot at the Fe-rich end of the OG field.

In summary there appears to be a progressive trend, from less evolved (Fe-rich, alkali-depleted,) to more evolved members (Fe-poor, alkali-enriched) from the EAFT to the RHEOR, and from each pair OG-OAFT and EG-RHEOR. These results tend to confirm the field and petrographic evidence that the OG is the parent rock of the OAFT rocks, whereas the EG could be the parent rock of the RHEOR rocks. Less certain is the origin of the EAFT, but conceivably it could derive from deeper sectors, or, less evolved portions of the OG magma chamber. Alternatively, EAFT rocks could have derived from a hybrid magma of near-tonalitic composition.

Results of six new chemical analyses of subvolcanic rocks

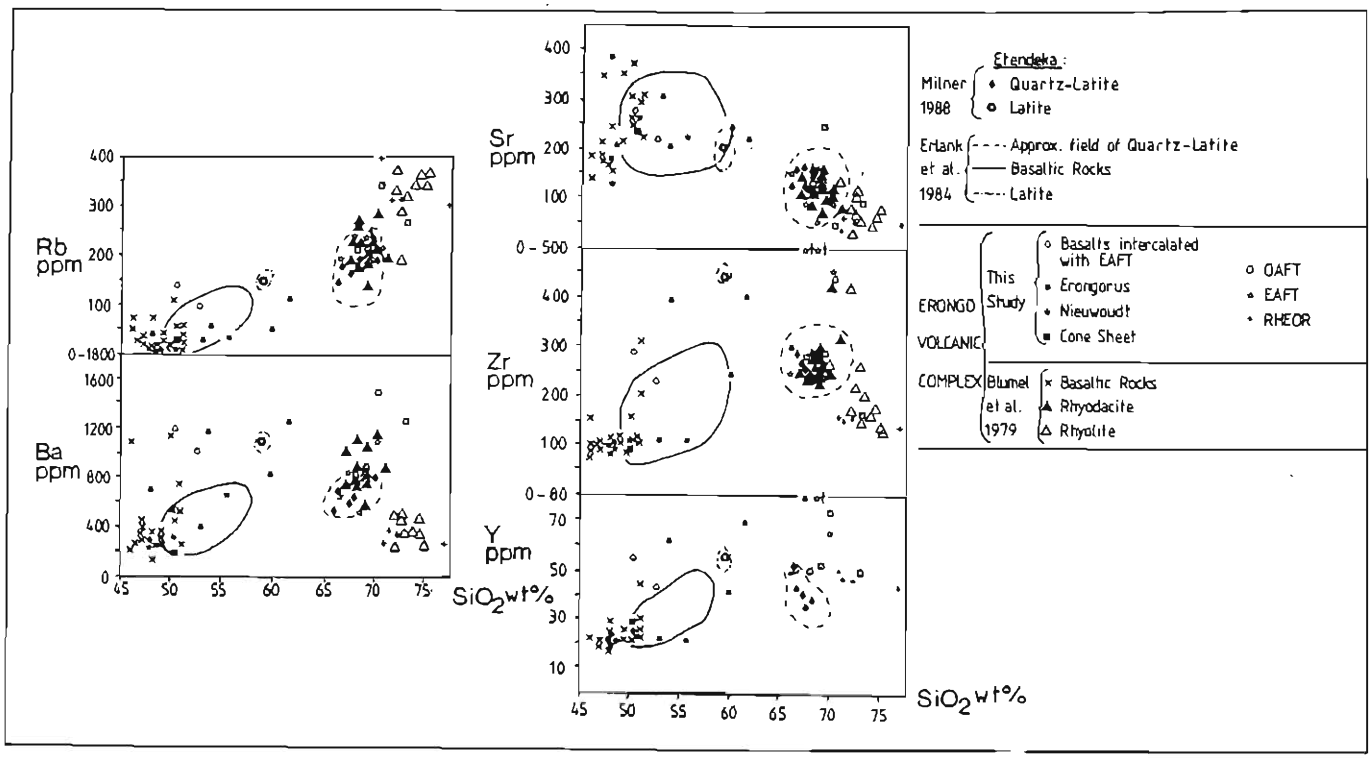

Figure 9 Diagrams showing plots of EVC rocks in terms of their SiO_2 versus selected trace elements (Rb, Ba, Sr, Zr, and Y). Quartz-latite, latite and basaltic rocks from the Etendeka Formation are plotted for comparison (data from Erlank *et al.*, 1984 and Milner, 1988).

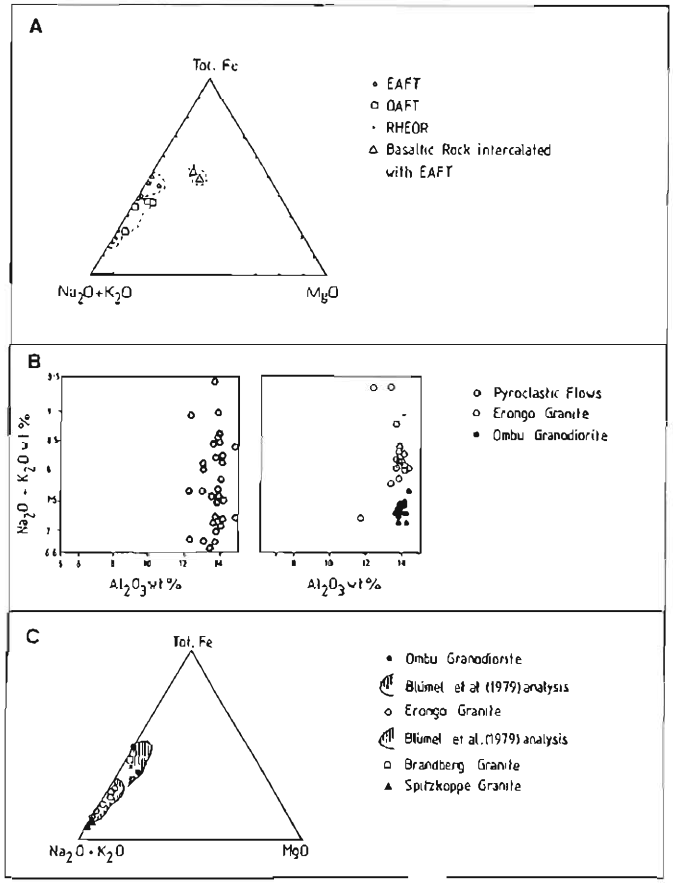

Figure 10 (A) Ternary (AFM) plot showing compositional variations of the EVC pyroclastic sequences. (B) Al_2O_3 versus Na_2O + K_2O plots of the EVC pyroclastic and cogenetic subvolcanic rocks. (C) Ternary (AFM) plot showing compositional variations of EVC subvolcanic rocks. Analyses of Brandberg hornblende-granite and Spitzkoppe granite are included for comparison. Compare this AFM plot with that in A and note correspondence of Erongo granite with RHEOR rocks and of Ombu granodiorite with OAFT rocks. Diagrams B and C incorporate analytical data from Blümel *et al.* (1979).

(OG and EG) are given in Table 4. Both OG and EG have a peraluminous chemistry (Al_2O_3 / Na_2O + K_2O + CaO > 1). A plot of alkalies versus alumina shown in Figure 10B indicates that both the OG and EG correspond well with the chemistry of the pyroclastic flows, with the former being slightly more alumina enriched. The AFM ternary diagram, shown in Figure 10C, incorporates geochemical data published by Blümel *et al.* (1979), as well as unpublished analyses from the Brandberg granite complex and the Spitzkoppe granites to the south-west of the EVC (Figure 1B). From this diagram it can be seen that the OG is enriched in Fe and Mg with respect to the EG and is similar to the Brandberg granite, whereas the EG has a more evolved chemistry, being richer in alkalies. The Spitzkoppe plutons are even more enriched in alkalies than the EG. The plots, shown in Figure 11, compare the OG and EG with A-type, I-type and Bushveld acid rocks. Except for Ga, the Rb, Ce, Zr, Zn, Y, and Nb contents of the EVC subvolcanic rocks seems to indicate that they are similar to the Bushveld acid rocks (granite and Rooiberg felsite, Twist & Harmer, 1987).

Table 3A Major and trace elements analyses of EAFT sequence rocks.Major elements expressed in weight per cent, trace elements in parts per million. Ee1(T) are ash-flow tuffs and Ee1(B) are basaltic lavas at the base of the sequence in the Brabant area. Ee2 are ash-flow tuffs at the top of the sequence in the same area. Analytical techniques as in Table 1. ND = not determined. -- = not detected

Sample No	ER227B	AZ8913	ER227C	AZ8981	AZ9057B	AZ8983
Type	Ee1(T)	Ee1(T)	Ee1(B)	Ee1(B)	Ee2	Ee2
SiO_2	68,53	66,37	50,27	52,59	67,49	70,27
TiO_2	0,64	0,98	2,29	1,50	0,71	0,50
Al_2O_3	12,72	14,14	14,69	15,73	13,13	11,96
Fe_2O_3	0,85	1,05	1,52	1,70	0,87	0,85
FeO	6,12	5,27	10,94	8,50	6,27	4,27
MnO	0,07	0,12	0,16	0,20	0,07	0,06
MgO	0,00	1,02	4,10	4,71	0,04	0,00
CaO	1,82	2,41	6,76	5,41	1,60	1,16
Na_2O	2,03	2,78	3,21	3,18	2,02	2,22
K_2O	5,14	4,07	2,09	3,00	5,68	5,61
P_2O_5	0,21	0,37	0,57	0,37	0,22	0,18
Cr_2O_3	0,02	0,06	0,02	0,07	0,01	0,05
H_2O-	0,15	ND	0,27	ND	0,25	ND
LOI	0,76	0,83	1,89	2,61	0,89	1,24
Total	99,06	99,47	98,78	99,57	99,25	98,37
Zn	139	103	512	137	143	122
Cu	21	15	33	21	19	11
Ni	13	10	40	65	6,1	--
Co	3,5	6	51	29	11	--
Ga	24	24	26	18	29	22
Mo	23	--	6,4	--	17	5
Nb	30	24	22	14	27	21
Zr	749	249	290	234	651	449
Y	91	52	55	44	85	65
Sr	55	152	271	220	90	92
Rb	235	192	141	101	236	216
U	11	--	--	--	4,6	4
Th	34	18	3,1	--	27	25
Pb	31	24	129	7	34	17
Ba	442	677	1202	1028	813	1072
Sc	0,6	23	28	42	15	--
Nd	63	39	6,5	49	17	67
Ce	111	57	29	104	60	119
La	5,8	61	28	--	29	73
S	4755	90	2441	320	88	560
Cl	ND	600	ND	380	ND	30
F	ND	2400	ND	750	ND	1660

The Ga content on the other hand agrees with the A-type field as defined by Collins *et al.* (1982). In this respect some overlap between the A and I fields is also observed in respect of the Nb and Y contents. The high Ga content and its ratio with Al_2O_3 are considered significant by Collins *et al.* (1982). They reason that because Ga is generally excluded from the anorthite structure relative to Al and because the An-rich plagioclase is preferentially retained in the restite source regions, melts derived from this region would have

Table 3B Major and trace elements analyses of OAFT sequence rocks. Major elements expressed in weight per cent oxide, trace elements in part per million. Eo1(V) vitrophyric base of cooling unit; Eo1(FB) flow banded crystal tuff; Eo1 crystal tuff. Analytical techniques as in Table 1. ND = not determined; -- = not detected

Sample No	AZ8994	AZ8995	AZ8955	AZ8960
Type	Eo1(V)	Eo1(FB)	Eo1(FB)	Eo1
SiO_2	69,11	68,09	73,07	70,28
TiO_2	0,80	0,70	0,39	0,53
Al_2O_3	13,80	13,73	13,57	12,32
Fe_2O_3	0,77	0,76	0,35	0,89
FeO	3,86	3,82	1,97	4,44
MnO	0,09	0,09	0,02	0,09
MgO	0,78	0,73	0,32	0,00
CaO	1,08	1,63	0,30	0,37
Na_2O	2,30	2,41	1,94	0,57
K_2O	4,89	4,62	5,78	8,96
P_2O_5	0,43	0,28	0,16	0,19
Cr_2O_3	0,06	0,04	0,04	0,07
LOI	1,48	1,83	2,12	1,53
Total	99,45	98,73	100,03	100,24
Zn	101	93	52	38
Cu	12	11	7	6
Ni	10	7	11	3
Co	6	4	4	--
Ga	23	20	18	26
Mo	3	5	--	5
Nb	15	14	14	23
Zr	277	282	160	456
Y	53	51	50	74
Sr	247	135	97	50
Rb	217	216	268	346
U	3	ND	9	ND
Th	21	19	11	26
Pb	29	34	35	15
Ba	869	813	1265	1519
Sc	6	ND	ND	26
Nd	40	33	75	72
Ce	120	93	96	145
La	0	59	41	157
S	1940	1090	ND	780
Cl	410	ND	ND	150
F	1600	1670	ND	1280

Table 3C Major and trace element analyses of RHEOR rocks (Egrh). Major elements expressed in weight per cent oxide, trace elements in parts per million. AZ 9063 A and B are from the Bersig area; AZ 9021 and 9023 are from Ekuta. ND = not determined. -- = not detected

Sample No	AZ9063A	AZ9063B	AZ9021	AZ9023
Type	Egrh	Egrh	Egrh	Egrh
SiO_2	70,70	76,85	71,36	72,28
TiO_2	0,28	0,25	0,27	0,32
Al_2O_3	15,63	13,56	13,07	13,34
Fe_2O_3	0,21	0,20	0,34	0,37
FeO	1,55	1,45	1,70	1,86
MnO	0,02	0,02	0,04	0,08
MgO	0,05	0,08	0,09	0,21
CaO	0,62	0,61	0,65	0,41
Na_2O	3,82	3,63	3,06	3,24
K_2O	5,29	3,45	4,79	5,27
P_2O_5	0,39	0,31	0,37	0,33
Cr_2O_3	0,01	0,02	0,05	0,04
H_2O-	0,12	0,17		
LOI	0,65	0,93	1,69	1,79
Total	99,34	101,53	97,48	99,54
Zn	37	50	78	187
Cu	5,8	4,3	5	5
Ni	7,1	8,9	0	5
Co	5	5,3	5	3
Ga	28	21	21	20
Mo	3,2	2,9	--	--
Nb	18	17	15	16
Zr	160	145	155	155
Y	53	44	48	47
Sr	50	52	67	60
Rb	399	296	312	317
U	9,3	7,6	--	3
Th	15	14	11	10
Pb	19	20	26	38
Ba	223	223	381	366
Sc	15	12	5	--
Nd	35	42	22	28
Ce	20	25	48	23
La	29	28	--	--
S	5336	292	3980	1950
Cl	ND	ND	30	340
F	ND	ND	1420	1240

high Ga / Al ratios. This could be the case for the OG and EG.

Major and trace element analyses of the undersaturated alkaline intrusive rocks are given in Table 5. On the basis of the geochemical nature of these rocks Patel (1988) concluded that the basanite represents a primitive magma characterised by high concentrations of MgO, total Fe, CaO, TiO_2, Co, Cr, V, Zn, Sr, Ba, Y, Nb, and Zr, low concentrations of K_2O, Al_2O_3, Na_2O and trace elements, such as Rb, Pb, and Th, and low K / Rb ratios (197–292).

The tephritic and phonolitic rocks show overall geochemical features that are consistent with more evolved magmas. These features can be summarised as follows: (1) depletion in MgO, CaO, total Fe, TiO_2, V, Co, Cu, Ba, Sr; and (2) enrichment in K_2O, Al_2O_3, Na_2O, Rb, Th, Pb, Zr, and higher K / Rb ratios (312–386), than the basanites.

Hydrothermal alteration and mineralisation

Introduction

A number of W-F-Sn, W, Be, Sn, F, and U occurrences are present on the northern side of the EVC, and their position is

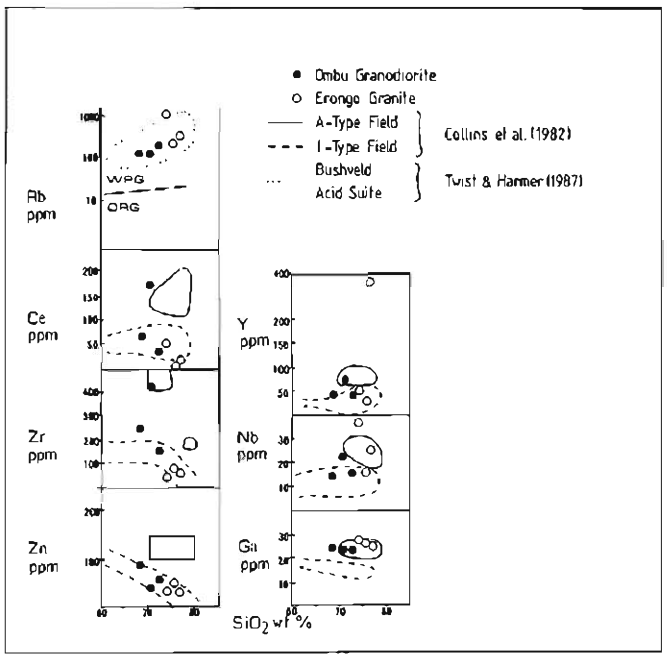

Figure 11 Diagrams showing plots of trace element (Rb, Ce, Zr, Zn, Y, Nb, Ga) versus the silica content of Erongo granite and Ombu granodiorite. Compositional fields of A- and I-type granitoids from eastern Australia (Collins *et al.*, 1982) and of Bushveld acid suite (Rb diagram only, data from Twist and Harmer, 1987) are indicated.

shown in Figure 2. The majority are spatially and genetically related to the Erongo granite. Some F occurrences are found within the OAFT units and are related to fumarolic activity. Unmineralised quartz-tourmaline veins occur along the western boundary of Ekuta, cutting OAFT rocks. Small areas of greisen and sericitic alteration with minor topaz disseminations are present in the western portion of Otjimisauna (Figure 2).

The Etemba-Anibib Sn and Be occurrences

Be and Sn mineralisation, hosted by a quartz-albite rock with numerous tourmaline veins and nests, is present in the Etemba farm. This mineralisation is associated with quartz-muscovite (greisen) alteration containing minor cassiterite disseminations. Drusy pegmatitic pods with crystals of beryl and tourmaline are also present. The quartz-albite rock is probably a high level (cupola) facies of the EG. Rocks around the mineralised locality are brecciated and are cut by veins of tourmaline, attesting to hydraulic fracturing induced by B-rich fluids.

About 1km west of the Be-Sn occurrence a northwest-trending fracture dips 75° to the southwest, and occurs in Damaran granite. This mineralised fracture is about 50m long and contains a core of quartz-sericite with symmetrical bands of quartz-tourmaline rock. Wolframite is present within the quartz-sericite material.

On the farm Anibib, along the contact zone between Erongo granite and granitic rocks of Pan-African age, there is intense brecciation and tourmalinisation associated with albitisation. Assays carried out by a mining concern during prospecting activities in this area showed the following values: 400–500 ppm W, about 2,5% F and 1000–10000 ppm Sn (J.E.Potgieter, pers. comm. 1986).

Table 4 Major and trace element analyses of subvolcanic rocks. Major elements expressed in weight per cent oxide, trace element in parts per million. Samples AZ 8942 A and B, 8945 B are from the Ombu granodiorite; samples AZ 9026, 8767, 8768 are from the Erongo granite. Analytical techniques as in Table 1. ND = not determined; -- = not detected

Sample No	AZ8942B	AZ8942A	AZ8945B	AZ9026	AZ8767	AZ8768
SiO_2	68,76	70,79	72,66	74,03	75,61	76,77
TiO_2	0,71	0,51	0,31	0,01	0,15	0,04
Al_2O_3	14,34	11,49	13,55	14,18	12,40	12,90
Fe_2O_3	0,71	1,14	0,43	0,23	2,01	0,18
FeO	3,96	5,70	2,13	1,16	ND	0,92
MnO	0,09	0,04	0,04	0,03	0,03	0,02
MgO	1,19	0,00	0,38	0,00	0,19	0,00
CaO	1,79	0,45	0,74	0,18	0,52	0,59
Na_2O	2,54	1,92	2,82	2,78	2,97	3,41
K_2O	4,80	5,19	5,72	5,02	5,45	4,58
P_2O_5	0,27	0,40	0,23	0,39	0,25	0,15
Cr_2O_3	0,06	0,05	ND	0,09	ND	0,08
LOI	0,54	1,94	1,46	1,15	0,50	0,62
Total	99,76	99,62	100,47	99,25	100,08	100,26
Zn	85	41	53	36	50	29
Cu	11	16	14	--	4	--
Ni	17	5	4	10	5	14
Co	7	--	6	4	4	--
Ga	24	24	20	35	32	25
Mo	--	5	3	--	2	--
Nb	14	23	16	37	15	25
Zr	224	421	151	41	83	56
Y	41	71	41	52	28	385
Sr	142	104	78	24	35	16
Rb	189	204	354	1024	398	598
U	8	3	6	--	6	14
Th	15	27	15	23	11	18
Pb	33	18	26	10	28	18
Ba	747	1619	306	132	ND	20
Sc	1	17	5	6	ND	--
Ce	66	170	32	54	--	17
Nd	44	90	15	12	0	29
La	--	129	44	--	27	30
Sn	19	--	44	14	43	28
W	--	--	5	--	--	36
Se	--	--	5	--	--	--
As	--	--	3	7	--	--
Ta	--	--	5	--	--	--
S	ND	7000	ND	3650	ND	1220
Cl	226	130	27	810	281	750
F	100	1800	130	8820	2070	5770
Rb/Sr	1,33	1,96	4,54	42,67	11,37	37,38

Krantzberg W-F-Sn deposit

The Krantzberg mine was a major tungsten producer in

Table 5 Major and trace element analyses of undersaturated alkaline intrusives. Major elements expressed in weight per cent oxide, trace elements in part per million. Samples 1 and 7 are tephriphonolites; 2,3 and 8 are tephrites; 10 is a phonolite; 5 and 6 basanites; 4 is phonotephrite. Analyses performed by XRF at Rhodes University (analyst S.Patel). -- = not detected

Sample No	1	2	3	4	5	6	7	8	9	10
SiO_2	48,970	44,54	44,14	46,52	38,86	41,32	50,67	42,22	41,710	52,600
TiO_2	0,790	1,75	1,75	1,27	2,52	2,50	0,58	1,49	1,430	0,450
Al_2O_3	21,140	16,29	17,30	18,32	14,83	13,59	21,60	15,29	22,650	22,060
Fe_2O_3	6,380	10,02	9,73	9,01	10,07	10,84	6,02	10,09	8,470	5,580
FeO	0,000	0,00	0,00	0,00	0,00	0,00	0,00	0,00	0,000	0,000
MnO	0,210	0,24	0,23	0,24	0,23	0,27	0,20	0,24	0,160	0,220
MgO	1,480	5,69	5,07	3,36	7,03	7,05	1,39	7,87	3,980	0,650
CaO	4,810	10,68	10,47	7,83	14,11	11,13	3,77	11,85	9,480	2,780
Na_2O	6,580	5,86	6,42	6,55	5,28	5,11	8,03	6,84	9,040	8,830
K_2O	4,760	3,55	4,01	4,06	1,07	2,34	5,51	2,91	4,460	6,130
P_2O_5	0,540	0,97	1,10	1,05	1,55	1,93	0,58	1,17	1,480	0,240
LOI	3,680	0,63	0,96	1,16	4,29	3,71	1,46	0,49	0,140	0,005
H_2O-	0,252	0,11	0,07	0,25	0,21	0,15	0,16	0,16	0,090	0,100
Total	99,580	100,32	101,23	99,62	100,06	99,96	99,95	100,63	103,091	99,650
Co	17	38	35	29	39,0	39	17	44	31	12
Cr	4	102	54	18	95,0	166	8	258	26	8
V	94	242	232	171	267,0	232	58	226	254	28
Zn	89	91	85	90	96,0	124	85	84	125	50
Cu	28	85	120	69	142,0	85	42	144	32	52
Ni	7	63	57	29	72,0	93	13	162	6	47
Zr	250	219	194	214	367,0	494	261	175	96	269
Nb	209	197	205	224	398,0	271	198	190	96	196
Rb	124	94	86	108	45,0	67	157	67	86	184
Sr	1463	1333	1339	1661	2111,0	2038	1328	1469	1418	888
Y	20	31	29	29	34,0	36	17	28	21	17
Ba	2213	1922	2261	2071	2354,0	2229	1775	2321	1326	1507
Pb	7	6	3	8	0,3	4	13	5	--	14
Th	20	16	19	18	9,0	13	26	13	--	42

Namibia. Mining operations ceased in 1979 and subsequent exploration did not result in economically feasible grades and tonnages. Cloos (1911) and Haughton *et al.* (1939) first reported on the Krantzberg deposit. Recently, this mineralised area was studied by Pirajno & Schlögl (1987). Mineralisation at Krantzberg consists of W (ferberite), F (fluorite), minor Sn (cassiterite), Be (beryl), Mo, Fe, and Cu sulphides. This mineralisation is hosted in replacement-type greisen rocks and quartz-tourmaline breccias.

The style of the Krantzberg deposit is shown in Figure 12E. The 'Krantzberg' is a prominent hill of Damaran rocks, which were protected from erosion by an overlying cap of Karoo clastic sediments and an outlier of EVC basaltic rocks (Figures 1B and 2). There are three main zones of alteration-mineralisation (Koppie Zone, Greisen Veins, and C-Zone), as well as a number of Sn-bearing tourmaline breccias. The C-Zone and Koppie Zone are formed by the greisenisation of Damaran granites. It is thought that hydrothermal fluids ascended from the subsurface apical portions of fractionated Erongo granite cupolas. The fluids were B- and F-rich and induced extensive selective replacement of pre-exisisting granite lithologies by quartz, sericite, topaz, and tourmaline. Late-stage veins contain ore minerals such as ferberite, scheelite, and minor sulphides. Breccia bodies on the southeast slopes of the Krantzbdrg contain fragments of volcanic rocks cemented by quartz and tourmaline. Cassiterite occurs as fine disseminations or as patches along the periphery of the breccia bodies. These breccias are interpreted as a type of hydraulic fracturing due to streaming of B-rich volatiles.

Uranium

Low-grade U mineralisation occurs in the Erongo granite plutons, particularly in the northwest and southwestern areas. Secondary U minerals are associated with jointing in areas of primary U enrichment (Potgieter, 1987). It is probable that this mineralisation is due to oxidising meteoric waters that have leached U from the fresh Erongo granite rock in areas of high permeability due to close-spacing jointing.

Fluorite and gold

Minor fluorite, mainly as disseminated crystals in vugs, and traces of Au (up to 100 ppb) locally occur in OAFT rocks in the Ekuta farm. Here the OAFT rocks are characterised by fumarolic alteration. Fumarolic pipes are also present and,

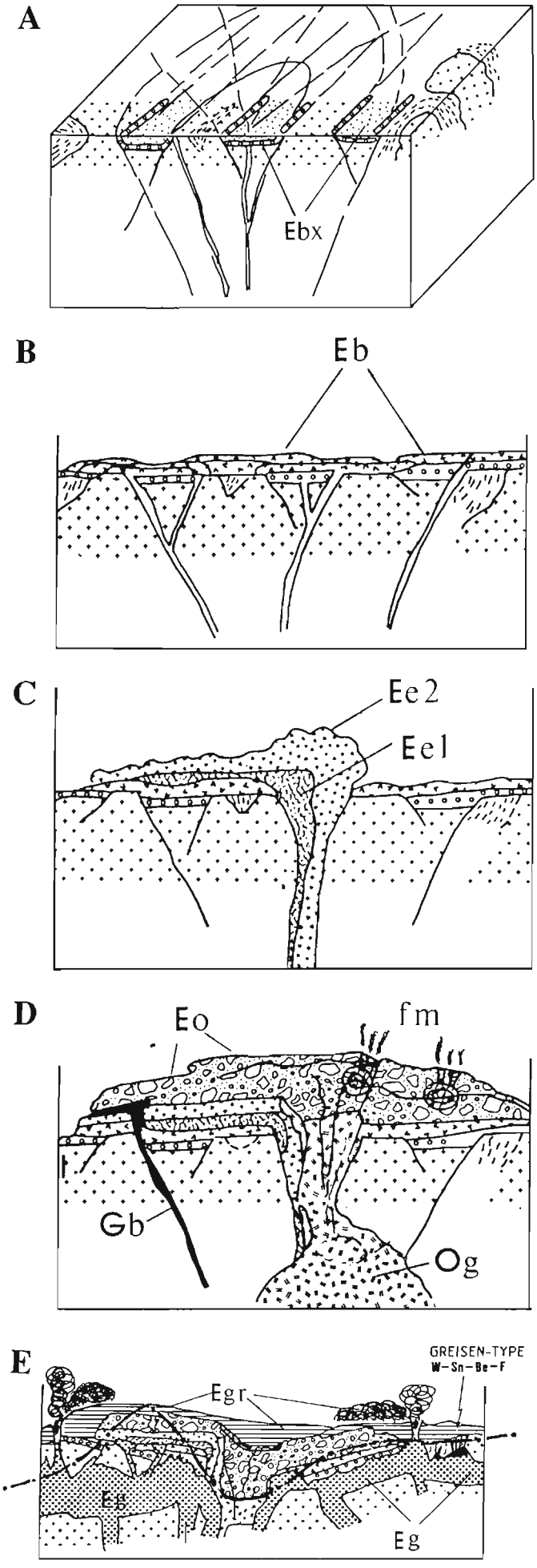

Figure 12 Schematic (not to scale), north-facing, diagrams depicting possible volcanic history of the EVC. (A) Block faulting of Damara basement (crosses = granite; small dashes = Kuiseb schist) and deposition of immature sediments (Ebx) in small grabens. Circular fractures may have developed due to pressures exerted by rising magmas. (B) Outpouring of basaltic lavas (Eb).(C) Erongorus event: eruption of EAFT units; basal sequence of intercalated lavas and ash-flow tuffs (Ee1), overlain by more evolved and crystal-rich units (Ee2). These pyroclastic flows were directed towards the north and west. (D) Ombu event: uprise and vesiculation of the Ombu granodiorite (Og) with large scale eruptions of ignimbrites of the OAFT sequence (Eo). Gabbroic rocks (Gb) were emplaced at the close of the EAFT event and early stages of OAFT event . Zone of fumarolic activity (fm). (E) Erongo event: intrusion of Erongo granite (Eg) around and below the volcanic structure. Possible venting of rheomorphic ash-flow tuffs (Egr, RHEOR rocks) and collapse of the volcanic edifice to form a caldera-like structure. Zone of greisen-type mineralisation are indicated by chemical symbols. Present-day erosion level shown by a dash-dot line.

therefore, it is likely that this area represents the upper portion of a thick OAFT cooling unit, within which vapour-phase alteration developed. Volatiles continuously exsolve from the pyroclastic material and tend to move upward through the pile of cooling units. The diffusion of these vapours (B, F, Cl, CO_2), or possibly H_2O, may result in the leaching of elements such as Si, Na, K, Fe, Ca, Cu, Pb, Zn, and perhaps Au and Ag.

The circulation and / or diffusion of fluids through ash-flow tuff cooling units several hundred metres thick may, therefore, produce epithermal-style mineral deposits. Two heat sources may be involved in driving a convection hydrothermal cell. One is the heat of the ash-flow units, and the other could be heat from the underlying subvolcanic intrusives. If abundant meteoric water is present, a geothermal system may be activated with hot springs and the development of quartz veins. Dry systems, poor in H_2O but otherwise enriched in other volatiles such as B, F, Cl, and CO_2, are indicated by the presence of minerals such as tourmaline, fluorite, alkali feldspar, chlorite, and the general lack of quartz veining. This appears to be the case for the EVC.

Volcanic history and discussion

A model showing a possible sequence of volcanic events that formed the EVC is schematically depicted in the diagrams of Figure 12. The volcanic history of the EVC probably began soon after the inception of block faulting and the deposition of immature clastic sediments in an area of crustal instability, perhaps due to a combination of tectonic movements and pressure exerted by uprising magma (Figure 12A and B). Outpouring of basaltic lavas took place towards the end of the Jurassic (about 145 Ma), from a number of different feeders. The extrusion of the basaltic lavas was followed by a phase of felsic volcanic activity, characterised by voluminous eruptions of pyroclastic material (Figure 12 C–E). Apart from the somewhat ambiguous RHEOR rocks, no lava flows are associated with the pyroclastic rocks at the present level of exposure. The three pyroclastic sequences (EAFT, OAFT,

RHEOR) represent distinct events, which rapidly succeeded one another. This is indicated by the absence of intervening palaeosols and interbedded sediments. The oldest is the EAFT sequence, which began with a transitional episode characterised by alternate eruptions of mafic-intermediate lavas and thin sheets of ash-flow tuffs (Ee1 in Figure 12 C). With time the nature of EAFT volcanism became progressively more explosive and more acidic, with no more lava flows being erupted (Ee2 in Figure 12 C). The general character of the EAFT rocks indicates that they were volatile-rich and emplaced at high temperature. The EAFT volcanism can be envisaged as one of fairly dense pyroclastic material with short eruption columns and a small gas-thrust component, erupted in a fountain-like fashion. The movement of the pyroclastic flows was towards the west and the north from a hypothetical vent possibly situated somewhere in the Ombu area. A resurgence of mafic magmatism occurred towards the end of the EAFT event and the beginning of the OAFT event. This resulted in the emplacement of gabbroic sills and lavas at the contact between the two pyroclastic series. The fact that these mafic rocks are only found in the northwestern areas (Omandumba), confirms that the northern side of the EVC was an area of tectonic instability.

The Ombu event (OAFT sequence) is represented by a series of ignimbrite eruptions (Eo in Figure 12D). Outliers of OAFT units in the vicinity of Krantzberg, in the northeast, indicate that OAFT units must have had a greater areal extent than that inferred by the present-day exposures within the confines of the caldera-like structure. In the southern part of the EVC, the OAFT surrounds and grades into the Ombu granodiorite (OG). The OG occupies a postulated vent area, now forming the Ombu plains. OAFT rocks may have derived from a shallow magmatic chamber, from which central eruptions ensued. The eruption column was probably sub-Plinian in character, with a greater gas-thrust component than the EAFT columns. Nevertheless, the absence of air-fall pyroclastics suggest that the OAFT columns were only high enough to cause gravitational collapse resulting in pyroclastic flows. The absence of recognisable base surge deposits suggests that there was little or no interaction with groundwaters, and that the energy was entirely provided by the gas content of the magma. There must have been several individual flows to account for the present-day thickness of at least 500m. The pyroclastic flows accumulated rapidly and welded onto one another forming thick cooling units. Degassing of the cooling units resulted in fumarolic activity with alteration and localised mineralisation (mainly fluorite disseminations).

The emplacement of the Erongo granite (EG) took place at around 144 Ma (Rb-Sr whole rock age, Sr_i = 0,722646, McNeil, 1989). It is postulated that below the present surface the EG forms a continuous mass above and around subsided blocks of volcanic and basement rocks (Figure 12E). The EG is important from the metallogenic viewpoint because it acted both as heat engine and as source for hydrothermal fluids, which were H_2O-poor, but rich in alkalies, B, and F. Widespread metasomatism occurred with local greisen-type mineralisation containing W, Sn, F, and Be, hosted in the roof zones of the EG and in the surrounding country rocks.

The rheomorphic rhyolitic rocks (RHEOR), representing the third and final volcanic event, may be the effusive equivalent of the EG (Erongo event). If this is correct then the eruption of the RHEOR volcanics must have occurred from a ring fracture outside the central volcanic edifice. This ring fracture, at the present level of exposure is occupied by the EG (Figure 12E). Collapse of the volcanic edifice at about this time led to the formation of the caldera-like structure and the centripetal tilting of the rock units. Estimates, based on correlation between the bases of RHEOR units between their highest (Erongorus) and lowest (Bersig) points, suggest that a collapse of at least 500m may have occurred.

The question is posed here whether the RHEOR are lava flows or ash-flow tuffs. Although somewhat ambiguous, field and petrographic evidence tends to support a pyroclastic origin for the RHEOR rocks. Blümel *et al.* (1979) stated that the 'stratified' rhyolitic rocks of the EVC are essentially tuffs and ignimbrites. Ekren *et al.* (1984) ascribed the absence of pyroclastic textures in rheomorphic rhyolitic rocks to the high temperature of these materials, which allows their remobilisation as liquids after emplacement. They further contended that very hot ash-flow tuff can move *en masse* during the welding process, and this results in flowage textures, which would be difficult, if not impossible, to distinguish from flow-banded lavas. There is no doubt that flowage structures can develop in ash-flow tuffs, as this is commonly observed in the OAFT units, for which a pyroclastic origin is beyond question. However, the banding in the OAFT rocks is wider, convoluted, and does not show the very fine laminations observed in the RHEOR rocks.

Elsewhere in Namibia, the Etendeka Formation, in the northwest of the country, consists of a series of intercalated basaltic lavas, latite, and quartz latite. The southern portion of the Etendeka volcanic plateau has been studied by Milner (1988), who recognised that the quartz latite units are high temperature ash-flow tuffs. The quartz latites of the Etendeka Formation occur as voluminous (80 to 800km^3) sheet-like units, and according to Milner (1988) they display features of both rhyolite lavas and ash-flow tuffs. They are characterised by being featureless, devitrified, with basal and upper zones showing flow banding, vitrophyres, and breccias. Geothermometry based on pyroxene and plagioclase, indicates temperatures of crystallisation of 1000 to 1100°C (Milner, 1988). For the RHEOR rocks in the Erongo Complex the question is not satisfactorily resolved, because only a few erosional remnants remain and therefore the real extent of these units is not known. On present evidence, a model of emplacement as pyroclastic flows is favoured, as indicated by the strongly welded rheomorphic tuffs in the Eileen farm area.

The final stage in the EVC geological history was the emplacement of alkaline mafic dykes and the undersaturated mafic plugs that intrude the pyroclastic sequences in the northeastern areas. It is possible that this may represent a resurgence of alkaline mafic magmatism, due to re-activation of deep-seated fractures. The relevance of this late magmatism, in terms of petrogenesis, to the evolution of the EVC is not clear. Isotopic and detailed geochemical studies are necessary to further our understanding of the Erongo Volcanic Complex.

Acknowledgements

This work was partly funded by CSIR and Rhodes University grants. The author is grateful to Gold Fields Namibia Ltd. for logistic support throughout the course of field work in the Erongo mountains. In particular, thanks are due to Anton Esterhuizen, Pat Vickers, Volker Petzel and Louis Kruger for their continued support. The hospitality of Mr. and Mrs. Hinterholzer of Ekuta, Mrs. W. Koegel of Ameib, Mr. and Mrs. Mosich of Koedoberg and the Van Rhyn family (Nieuwoudt), is remembered with gratitude. Mrs. L. Wadeson draughted the illustrations and Dr. M. Diehl (Geological Survey of Namibia) and an anonymous referee are thanked for their constructive criticism of this paper.

References

Aldrich, S. (1986). Progress report on a gravity and magnetic investigation of the Messum and Erongo igneous complexes. *Communs. geol. Surv. SWA/ Namibia*,**2**,47–52.

Bernasconi, A. (1986). The Marinkas Kwela alkali intrusive - A porphyry molybdenum system of Cambrian age in southern South West Africa/ Namibia, 1587–1592. *In*: Anhaeusser, C.R. & Maske, S. (Eds.), *Mineral Deposits of Southern Africa*, I. Geol. Soc. S. Afr., 1020pp.

Blümel, W.D., Emmerman, R. & Huser, K. (1979). Der Erongo. Geowissens-chaffiche Beschreibung und Dentung eines südwestafrikamischen Vulkancomplexes. *Scient. Res. SWA Ser., S.W.Africa scient. Soc.*, **16**, 140pp.

Cas, R.A.F. & Wright, J.V. (1987). *Volcanic Successions: Modern and Ancient: a Geological Approach to Processes, Products and Successions*. Allen & Unwin, London, 528pp.

Cloos, H. (1911). Geologische Beobachtungen in Südafrika. II. Geologie des Erongoim Hererolande. *Beitr. Geol. Erforsch. Deutsche Schutzgeb.*, **3**, 84pp.

Collins, W.J., Beams, S.D., White,A.J.R. & Chappell, B.W. (1982). Nature and origin of A-type granites with particualr reference to southeastern Australia. *Contr. Miner. Petrol.*, **80**, 189–200.

Ekren, E.B., Mcintyre, D.H. & Bennett, E.H. (1984). High-temperature, large volume, lava-like ash-flow tuffs without calderas in southwestern Idaho. *Prof. Pap. U.S. geol. Surv.*, **1272**, 73pp.

Erlank, A.J., Marsh, J.S., Duncan, A.R., Miller, R.MCG., Hawkesworth, C.J., Betton, P.J. & Rex, D.C. (1984). Geochemistry and petrogenesis of the Etendeka volcanic rocks from SWA/Namibia. *In*: Erlank, A.J. (Ed.), *Petrogenesis of the Volcanic Rocks of the Karoo Province*, 195–245. Spec. Publ. geol. Soc. S. Afr., **13**, 395pp.

Fisher, R.V. & Schmincke, H.U. (1984). *Pyroclastic Rocks*. Springer-Verlag, Berlin, 472pp.

Haughton, S.H., Frommurze, H.F., Geverg, T.H., Schwellnus, C.M. & Rossouw, P.J. (1939). The geology and mineral deposits of the Omaruru area, South West Africa. *Explan. Sheet 71, Geol. Surv. S. Afr.*, 15lpp.

Hegenberger, W. (1988). Karoo sediments of the Erongo Mountains, their environmental setting and correlation. *Commun. geol. Surv. SWAfrica/ Namibia*, **4**, 51–57.

Kujawa, T. (1986). *The petrography, genesis and associated mineralisation of the Erongo granite, Omaruru Hills, SWA/ Namibia*. BSc. Hons. Project (unpubl.), Univ. Cape Town, 53pp.

Le Maitre, R.W. (1984). A proposal by the IUGS subcommission on the systematics of igneous rocks for a chemical classification of volcanic rocks based on total alkali silica (TAS) diagrams. *Aust. J. Earth Sci.*, **31**, 243–255.

Lofgren, G. (1971). Experimentally produced devitrification textures in natural rhyolitic glass. *Bull. geol. Soc. Amer.*, **82**, 111-124.

Marsh, J.S. (1973). Relationship between transform directions and alkaline igneous rock lineaments in Africa and South America. *Earth Planet. Sci. Lett.*, **18**, 317–323.

---- (1987).Basalt geochemistry and tectonic discrimination within continental flood basalt provinces. *Volc. Geotherm. Res.*, **32**, 35–49.

Martin, H., Mathias, M. & Simpson, E.S.W. (1960). The Damaraland sub-volcanic ring complexes in South West Africa. *Rep. Internat. Geol. Congr. Copenhagen*, **13**, 155–174.

McNeil, G.W. (1989). *A geochemical study of three Namibian igneous complexes*. B.Sc. Hons. Project (unpubl.), Univ. St.Andrews, 57pp.

Milner, S. C. (1988). *The geology and geochemistry of the Etendeka Formation quartz latites, Namibia*. Ph.D. thesis (unpubl.), Univ. Cape Town,244pp.

Patel, S. (1988). *The petrology of the alkali intrusive rocks from the Erongo Volcanic Complex*. B.Sc. Hons. Project (unpubl.), Rhodes Univ., Grahamstown, 34pp.

Pichavant, M. (1981). An experimental study of the effect of boron on a water saturated haplogranite at 1 kbar vapour pressure. *Contr. Miner. Petrol.*, **76**, 430–439.

---- & Manning, D.C.A. (1984). Petrogenesis of tourmaline granites and topaz granites; the contribution of experimental data. *Physics Earth and Planet. Inter.*, **35**, 31-50.

Pirajno, F. & Jacob, R.E. (1987). Sn-W metallogeny in the Damara orogen, South West Africa/ Namibia. *S. Afr. J. Geol.*, **90**, 239–255.

---- & Schlögl, H.U. (1987). The alteration-mineralization of the Krantzberg tungsten deposit, South West Africa/ Namibia. *S. Afr. J. Geol.*, **90**, 499–508.

Potgieter, J.E. (1987). *Anorogenic alkaline ring-type complexes of the Damaraland province, Namibia, and their economic potential*. M.Sc. thesis (unpubl.), Rhodes Univ., Grahamstown, 150pp.

Prins, P. (1981). The geochemical evolution of the alkaline and carbonatite complexes of the Damaraland Igneous Province, South West Africa. *Ann. Univ. Stellenbosch* **Ser. A1(3)**, 145–278.

Siedner, G. & Miller, J.A. (1968). K-Ar age determinations on basaltic rocks from South West Africa and their bearing on continental drift. *Earth Planet. Sci. Lett.*, **4**, 451–458.

Smithies, R.H. (1988). The formation of tourmaline nests within leucogranites and possible relationship to hydrothermal W/Sn mineralisation. *Ext. Abstr. Geocongr. '88*, Univ. Natal, Durban, 591–594.

Streckeisen, A. (1976). To each plutonic rock its proper name. *Earth Sci. Rev.*, **12**, 1–33.

Twist, D. & Harmer, R.E.J. (1987). Geochemistry of contrasting siliceous magmatic suites in the Bushveld Complex: genetic aspects and implications for tectonic discrimination diagrams. *J. Volc. Geotherm. Res.*, **32**, 83–98.

Viljoen, R.P., Minnitt, R.C.A. & Viljoen, M.J. (1986). Porphyry copper-molybdenum mineralization at the Lorelei, South West

Africa/ Namibia, 1559-1566. *In*: Anhaeusser, C.R. & Maske, S. (Eds.), *Mineral Deposits of Southern Africa, II*. Geol. Soc. S. Afr., 1020pp.

Watson, N.I. (1982). *Regional geology of areas 2115C and 2115DC*. Unpubl. Rep. Geol.Surv. SWA/ Namibia.

Winchester, J.A. & Floyd, P.A. (1976). Geochemical magma type discrimination: application to altered and metamorphosed basic igneous rocks. *Earth Planet. Sci. Lett.*, **28**, 459–469.